Applying Season-ahead Streamflow Forecasts to Guide Reservoir Allocations for the Highland Lakes in Central Texas

By

Matthew Grzegorzewski

A thesis submitted in partial fulfillment of

the requirements for the degree of

MASTER OF SCIENCE

CIVIL AND ENVIRONMENTAL ENGINEERING

At the

UNIVERSITY OF WISCONSIN-MADISON

Summer 2015

Acknowledgements

I would like to thank my graduate advisor Paul Block for his guidance and support during my time at the University of Wisconsin-Madison. I would also like to thank Dr. Steve Loheide and Dr. Chin Wu for serving as members of my committee and providing feedback on my research. A special thanks is given to the Lower Colorado River Authority, especially Ron Anderson, for all their insight into hydrologic forecasting, climate research, and river operations. Lastly, I owe a large part of my success to the moral support and assistance of Brian Zimmerman and the rest of the Water Systems & Society research group. This study was made possible by funding from the National Oceanic and Atmospheric Administration/Climate Program Office/Sectoral Applications Research Program (NOAA/CPO/SARP) (Sponsor Award Reference No.: NA13OAR4310153).

Abstract

Season-ahead reservoir inflow forecasts can assist water managers by anticipating and preparing for extreme conditions, such as droughts. Previous studies have developed statistical streamflow models, which rely on hydrologic persistence or large-scale climate variables. This study incorporates both, including local and global predictor information, in a novel hybrid autoregressive-principal component regression framework. A superior combination of predictors is obtained, based on select performance metrics, using both linear and logistic regression models. Application to the Lower Colorado River basin in Texas demonstrates significant overall skill, particularly for the March-June inflow season (correlation = 0.70; RPSS = 0.73) Evaluation of the July-October inflow season also exhibits increased predictive skill over climatology (correlation = 0.63; RPSS = 0.65.)

The prediction model outputs are subsequently coupled to a reservoir operations model to compare the impacts of incorporating a streamflow forecast into management policies versus simply applying long-term historical average. The two major reservoirs that provide water for the LCRB, Lake Travis and Lake Buchanan, are treated as a single water supply and a water balance model is created to simulate outflows (e.g. evaporation, water allocations, environmental demands) and actual inflows for the time period 1982-2010. Operating policies from the most recent revision of the Lower Colorado River Authority's Water Management Plan are used. Allocations are made based on reliability of maintaining combined storage in the reservoir above 1.3 million acre-feet, which

is the threshold for meeting extreme drought criteria within the current Water Management Plan. Results indicate some increased benefits with the forecast in both short and long-term operations, especially in response to extreme events.

Table of Contents

CHAPTER 1: Introduction

1.1 Motivation

Over the past century, droughts have had pronounced impacts on society, local economies, and the environment. From 1980 to 2003, severe droughts cost the United States $144 billion, making it the most costly type of natural disaster for this time period (Cook et. al., 2007). The early 2000's drought, which affected primarily the western United States, sparked the largest fires in the past century in the states of Oregon, Arizona, and California, burning nearly 1,000,000 acres (Cook et. al., 2007), and also caused insect outbreaks in the American Southwest, leading to the loss of over three million acres of ponderosa and pinyon pine (Clifford et. al., 2008). By April 2005, reservoir storage in Lake Powell, one of the largest reservoirs in the United States, had declined to 7.96 million acre-feet, or about 32% of total storage capacity (United States Bureau of Reclamation, Upper Colorado Region. Accessed May 2015, http://www.usbr.gov/uc/crsp/download/acre-feet-1434991611755.lst). Climate models predict that precipitation across parts of the United States, in particular the southern states, may decrease over the next 100 years leading to increased drought frequency (Karl et. al., 2009; Strzepek et. al., 2010). Thus water-dependent sectors are progressively seeking opportunities to mitigate year-to-year climate variability impacts through improved decision-making. The suite of options is broad, with no one-size-fits-all approach; however non-infrastructural alternatives such as season-ahead hydroclimatic forecasts are increasingly

attractive. Skillful forecasts can allow managers to optimally distribute precious water resources in an efficient and effective manner to improve reservoir management.

A systems approach towards water resources management allows water planners to consider both structural and nonstructural options to optimize decision-making. Traditionally, static rule curves have been used in regulating water releases. Long term operational decisions are thus dependent on existing storages and climatological averages of streamflow and offer water managers little flexibility to anticipate and respond to extreme events. The utility of season-ahead streamflow forecasts (SSFs) has been recognized for a long time (Changnon & Vonhamme, 1986) and SSFs have progressed and shown significant improvements in predictive skill over recent years, however their full implementation into decision support tools and operating procedures has not been widespread. Reasons for this include poor skill, inappropriate scale or spatial resolution, and lack of tailoring to suit the needs of management needs. There are notable exceptions. Pagano et. al, 2002 investigated how seasonal forecasts impacted water management in the American Southwest during the strong El Nino of 1997-1998, where certain water managers chose to release water in anticipation of floods. This advanced climate information led to an increase in hydropower production and revenue (Hamlet et. al., 2002). SSFs therefore have the potential for more informed decision-making that may lead to superior outcomes (Chiew et, al. 2003). Probabilistic SSFs can additionally help to identify climate and model uncertainty benefits (Krzysztofowicz, 2001; Ramos

et. al., 2013). Additional research linking predictions and decision models in an objective manner is warranted to further elucidate advantages and better understand the economic impacts of poor forecasts. Under drought conditions, managers often value mitigating losses over the current and subsequent seasons above marginal gains in long-term operations; SSFs have the potential to address exactly such preferences.

1.2 Research Objectives

The driving force behind the research for this thesis is droughts and their impacts on decision-making within water management. Research objectives for this project include:

-To analyze historical streamflow and reservoir inflow data and identify key water allocation decision points

-To assess the predictive skill of various local and global predictors for reservoir inflows

-To develop a statistical hydroclimatic forecast with a lead time of 3-6 months and determine most appropriate form (e.g. deterministic vs. probabilistic, level of complexity, number of variables, etc.)

-To evaluate effectiveness of model predictive skill with performance metrics

-To incorporate forecast into existing water management policies and compare simulations of reservoir operations and water allocations to using historical averages (i.e. climatology)

1.3 Lower Colorado River Basin

To illustrate the proposed hybrid prediction-modeling framework, the Lower Colorado River basin (LCRB) in Texas is selected as a case study (Figure 1).

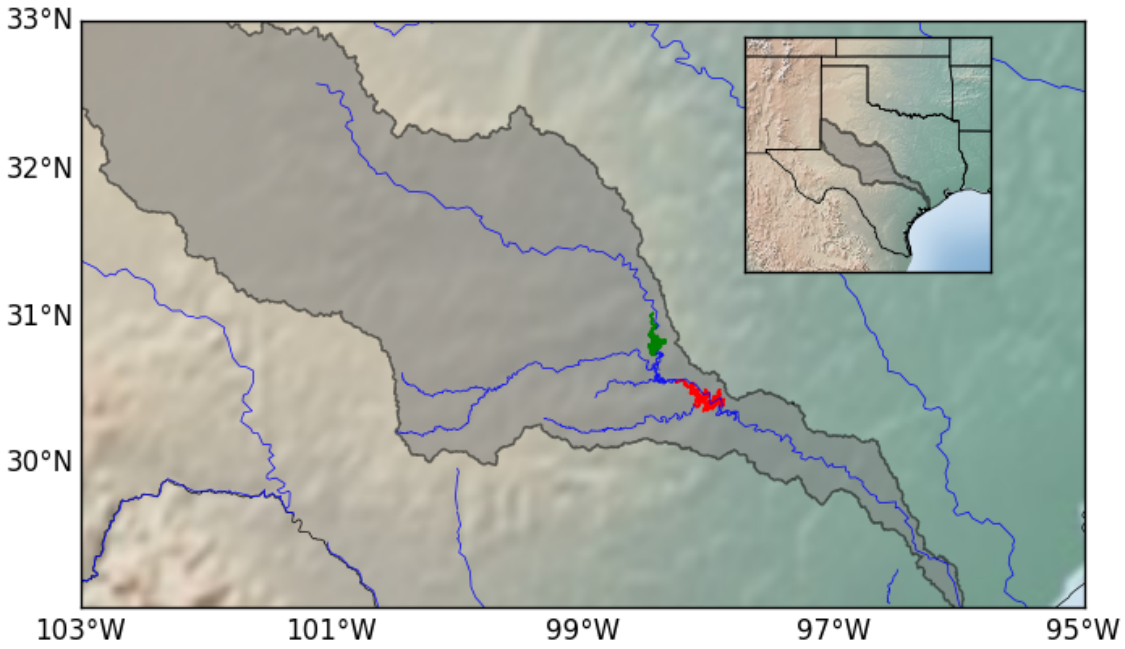

Figure 1: Colorado River basin in Texas with Lake Buchanan shown in green and and Lake Travis shown in red. The four major tributaries to the Highland Lakes are (from North to South): Colorado River, Llano River, Sandy Creek, and Pedernales River.

This watershed, and Texas in general, has endured severe drought conditions since approximately 2007. The Highland Lakes, a series of six dams and reservoirs in the basin, located northwest (upstream) of the city of Austin, TX, have seen reservoir levels drop precariously, to as low as 34% of total storage capacity (2.1 million acre-feet). The Lower Colorado River Authority (LCRA) is the institution responsible for managing the Lake Buchanan and Lake Travis reservoirs, which serve over one million people and numerous industries in the vicinity. The reservoirs were primarily built for flood control, as this region is

susceptible to extreme flash flooding events due to relatively shallow soils, steep terrain, and the primarily shrub and pasture land cover. Despite the notoriously dry conditions in recent history, the watershed has experienced extensive flooding in the past, such as the flooding event that brought an end to the drought of record in the 1950s, the Christmas flood of 1991, and the "rain bomb" of 2007 that brought 18 inches of precipitation to Marble Falls, TX within 6 hours (LCRA, 2007). Lake Travis has a flood pool with a storage capacity of 787,000 acre-feet, which is operated in accordance with US Army Corps of Engineers flood regulations. The reservoirs are also managed for various recreational activities, such as boating and fishing, maintaining a freshwater inflow into the Matagorda Bay estuary, and irrigated agriculture. Combined storage of the two major reservoirs dropped to one third of total storage capacity (2.01 million acre-feet) during the most recent drought, however recent heavy rains in the spring of 2015 have risen storage levels to 78% of total storage capacity, which may be signaling an end to extremely dry conditions (Figure 2)

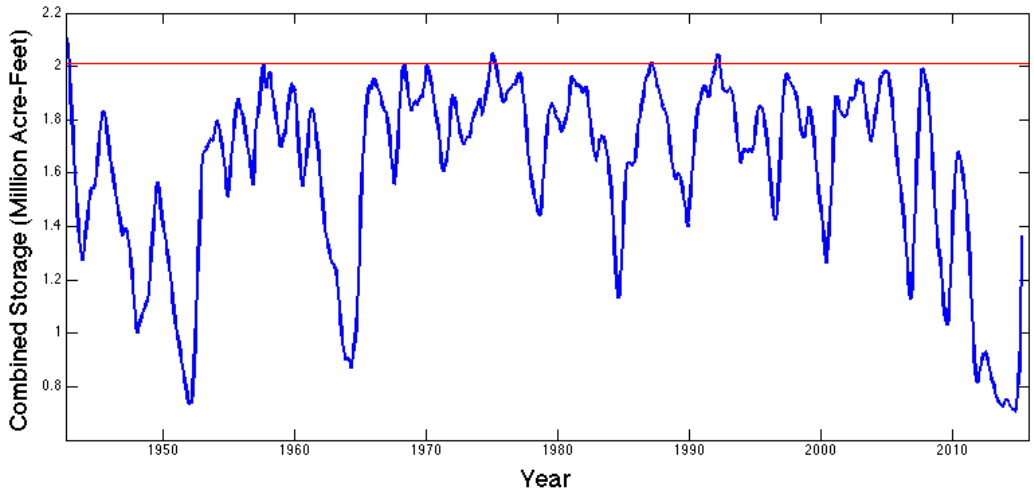

Figure 2: Combined Storage of Lake Travis and Lake Buchanan for 1940-2015. Horizontal red line is total storage capacity (2.01 million acre-feet)

Inflows to the reservoirs are highest in the months of May and June with a secondary peak in inflows occurring in the month of October (Figure 3).

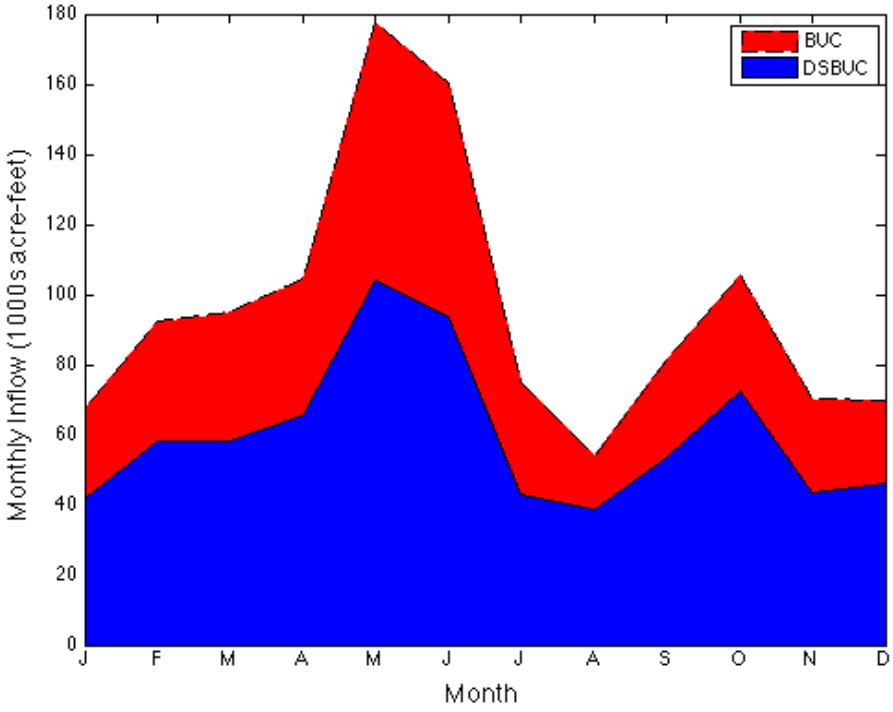

Figure 3: Average monthly reservoir inflows averaged over 1940-2013. Dashed line is total aggregate inflows, red area is fraction of total inflows to Lake Buchanan, and blue area is fraction of total inflows to Lake Travis.

However there is significant variability in the monthly inflows (Figure 4), which is largely driven by extreme events. At some point in the historical record, each month has represented the annual maximum monthly inflow at least once.

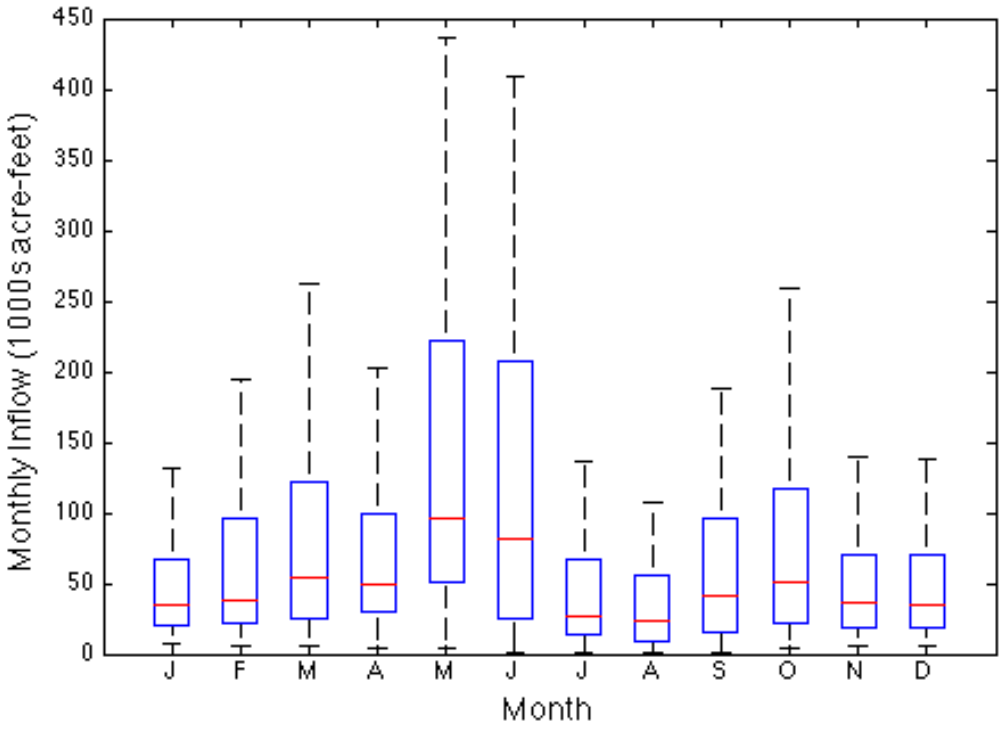

Figure 4: Boxplot of total aggregate monthly inflows to Highland Lakes

Inflow data was split into three seasons to align with key decision deadlines (evaluation dates) for irrigation water contracts for the LCRA (March 1 and July 1) and to capture both inflow peaks and the dry winter period: March-June (MAMJ), July-October (JASO), and November-February (NDJF). The LCRA is interested in evaluating season-ahead inflow forecasts to guide water allocation decisions for the MAMJ and JASO seasons, and are considering adopting such approaches into their revised Water Management Plan.

The LCRA has undergone several revisions of their Water Management Plan (WMP) for the LCRB ever since a court order in 1988 made one mandatory. The Texas Commission on Environmental Quality approved the first WMP in 1989. Several updates were approved in 1991, 1992, 1999, and 2010. Another

revision, which was submitted in October 2014, is currently in the process of being approved. The operating policies and Drought Contingency Plan from this most recent revision are used for this study. The WMP outlines water allocations for the two primary types of water customers within the LCRB: firm and interruptible. Interruptible customers are primarily three irrigation districts (Lakeside, Gulf Coast, and Garwood) and Pierce Ranch. Aside from Garwood, interruptible water allocations (IWAs) for these customers are issued as water contracts on a seasonal basis related to the two crop seasons, first crop season (March-June) and second crop season (July-October). Seasonal contracts for irrigation are issued based on existing water storage and the current water supply condition. Firm customers are based on long-term water contracts and have a higher priority on water. More information on firm customers is detailed in the Data section. During the most recent drought period, water supplies from interruptible customers have been completely cut off for four consecutive years (2012-2015).

1.4 Outline

The work for this thesis is divided into two major sections.

Chapter 2 focuses on development of the hybrid autoregressive-principal component regression model for forecasting reservoir inflows into the Highland Lakes. This chapter will focus on predictor selection and methods for model development. Cross-validated hindcast results are presented for two seasons, March-June and July-October.

Chapter 3 covers the application of the seasonal reservoir inflow forecast model in water management within the LCRB in a reservoir operation simulation. A background on water management plans within the LCRB is provided in this section along with procedures for the water balance model and for determining water allocations to irrigation. This section provides results of the simulations with restrictions from the latest revision of the water management plan along with results when the restrictions are removed.

Chapter 4 contains a summary of results.

CHAPTER 2: Hybrid Autoregressive-Principal Component Prediction Model

2.1 Background

2.1.1 Autoregressive Models

Autoregressive approaches have a long and rich history in modeling expected hydrological processes, particularly streamflow. (Loucks et. al., 1981; Salas, 1993; Box et. al., 2008) These models rely solely on persistence (memory) to predict streamflow rates, typically on shorter time-scales (e.g. hours, days), however successful applications on longer time scales, including monthly, seasonal, and even interannual have been illustrated (Mohan & Vedula, 1995; Yurekli et al., 2005; Gamiz-Fortis et. al., 2011; Can et al., 2012). More recently, autoregressive models have been coupled with large-scale climate variables, such as sea surface temperature (SST) information and climate indices (Gamiz-Fortis et. al., 2008; Adwallah & Rousselle, 2000). Sea surface temperature (SST) anomalies in the Nino 3.4 region have been well documented to affect climate and drought across the United States (Piechota and Dracup, 1996; Quan et. al., 2006).

2.1.2 Statistical and Dynamical Model Comparison

Statistical and dynamical modeling frameworks are commonly applied in hydroclimatic prediction. Statistical models focus solely on capturing relationships between exogenous predictors and hydroclimatic variables of interest (Garen, 1992). In the context of streamflow, predictors often account for two major sources of variability: antecedent watershed conditions and persistent climatic

influences. Dynamical models, in contrast, require hydrology, water balance, and energy equations to describe all physical climate and catchment processes, and are thus typically significantly more complex than statistical approaches. Dynamical models may be run in a predictive mode by utilizing expected hydro-meteorological conditions, but suffer from additional sources of uncertainty stemming from the many parameters required to capture climate and catchment dynamics. Statistical models are also not immune to drawbacks, and are most often limited by the availability of historical data. Additionally, care must be taken to prevent multi-collinearity between predictors and spurious correlations that can artificially inflate model skill. Nonetheless, statistical models remain appealing in streamflow prediction given less required input and physical data and reduced building and processing time as compared with their dynamical counterparts. (Coulibaly et. al., 2001; Wei & Watkins, 2011).

This thesis proposes a novel hybrid autoregressive-statistical streamflow prediction modeling framework that expands on a traditional Autoregressive Moving Average (ARMA) model by including both local and global predictor variables. Principal component analysis (PCA) is jointly applied to the ARMA outcomes and selected combinations of hydroclimatic predictors and subsequently regressed on streamflow. This technique merges persistent exogenous and endogenous predictive information, eliminates multicollinearity between predictors, and captures dominant hydroclimatic signals that may ultimately lead toward improved predictive skill.

2.2 Data Sources and Selection of Season-ahead Predictors

2.2.1 Reservoir Inflows

Monthly reservoir inflow data for 1940-2013 was obtained from the LCRA, based on USGS streamflow gages on the four major tributaries to the Highland Lakes: Colorado River, Llano River, Sandy Creek, and Pedernales River (Figure 1). Monthly streamflow measurements were adjusted with runoff factors provided by the LCRA to account for additional inflow downstream of each gage station. Adjusted streamflow is summed to produce total aggregate inflows to the Highland Lakes (all 4 tributaries), inflow to Lake Buchanan (Colorado River only), and inflow downstream of Buchanan (Llano River, Sandy Creek, and Pedernales River only.) Streamflow on the Colorado River is also adjusted for the 1990 construction of the O.H. Ivie reservoir in the upper part of the basin (LCRA , 2010).

2.2.2 Global Predictors

2.2.2.1 Climate Indices

Various local and global variables are evaluated as potential predictors for the regression model. Large-scale climate drivers, such as El Nino Southern Oscillation (ENSO), Pacific Decadal Oscillation (PDO), and Atlantic Multidecadal Oscillation (AMO), have been shown to contribute to precipitation variability and drought conditions in Texas (Piechota & Dracup, 1996; McCabe et. al., 2004; Rajagopalan et. al., 2000). Pre-season averages (November-February, March-June) of three representative indices, Nino 3.4 (e.g. SSTs in the equatorial

Pacific Ocean), PDO, and AMO, were obtained to gauge their predictive skill (NOAA Climate Prediction Center. Accessed March 2014, http://www.cpc.ncep.noaa.gov/data/indices/sstoi.indices; University of Washington, Joint Institute for the Study of the Atmosphere and Ocean. Accessed April 2014, http://research.jisao.washington.edu/pdo/PDO.latest; NOAA Earth System Research Laboratory. Accessed April 2014, http://www.esrl.noaa.gov/psd/data/correlation/amon.us.long.data). Pearson correlations between the NDJF Nino 3.4, PDO and AMO indices and the MAMJ inflow season are 0.24, 0.18, and -0.16, respectively. Correlations between the three MAMJ climate indices and JASO inflows are noticeably weaker at 0.09, 0.11, and -0.08, respectively.

2.2.2.2 Sea Surface Temperatures

Given that these large-scale global phenomena are conditioned on sea-surface temperatures (SST) and sea-level pressures (SLP), and that regions of highest correlation may not perfectly align with the indices as defined (Morin et. al., 2008), global monthly gridded SST (2°x2°) and SLP (2.5°x2.5°) data from NOAA Extended Reconstructed V3b and NCEP/NCAR Reanalysis, respectively, are evaluated (Kalnay et. al., 1996; Smith et. al., 2008). Many studies associate SST and SLP with precipitation and drought patterns in North America and Texas (e.g. Ting & Wang, 1997; Zhang & Mann, 2005; Hoerling et. al., 2012). Initially, inflows are correlated with global gridded SSTs from the preceding season and statistically significant (significance level of 0.03) grid points in the Atlantic and Pacific Oceans are identified as potential predictors. SST grids clustered in a

region are averaged and normalized to form a single average SST value. For the MAMJ season, four candidate NDJF SST regions are identified; three correlate positively with inflow (0.30, 0.42, and 0.43) and one negatively (-0.36) (Figure 5a.) For the JASO season, five candidate MAMJ SST regions are identified; three correlate positively with inflow (0.32, 0.33, and 0.36) and two negatively (-0.30 and -0.40) (Figure 5b.) Regions are selected based on proximity to Texas and the findings of previous studies identifying regions of physical relevance (Rajagopalan et. al., 2000, Tootle & Piechota, 2006).

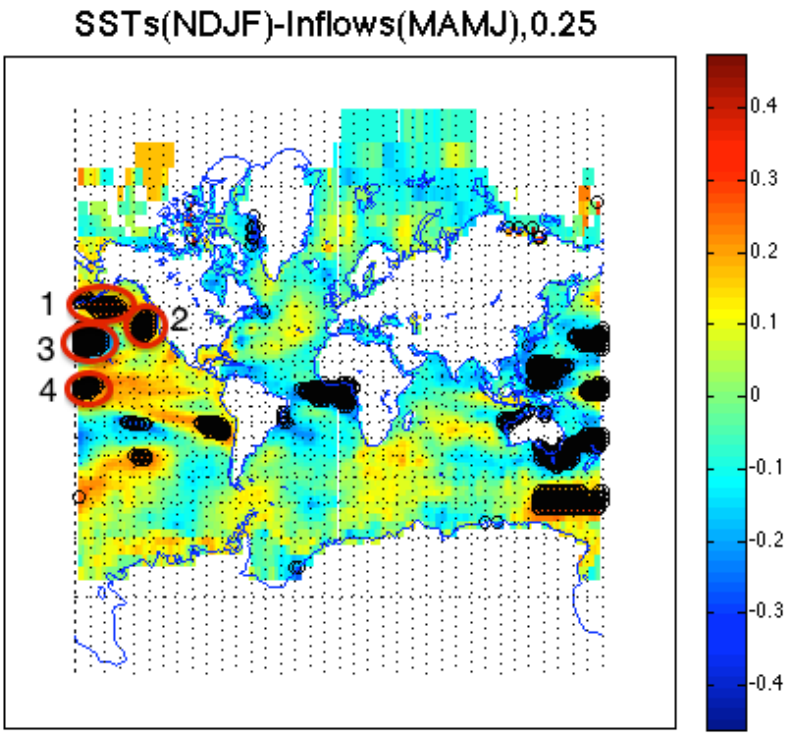

(a)

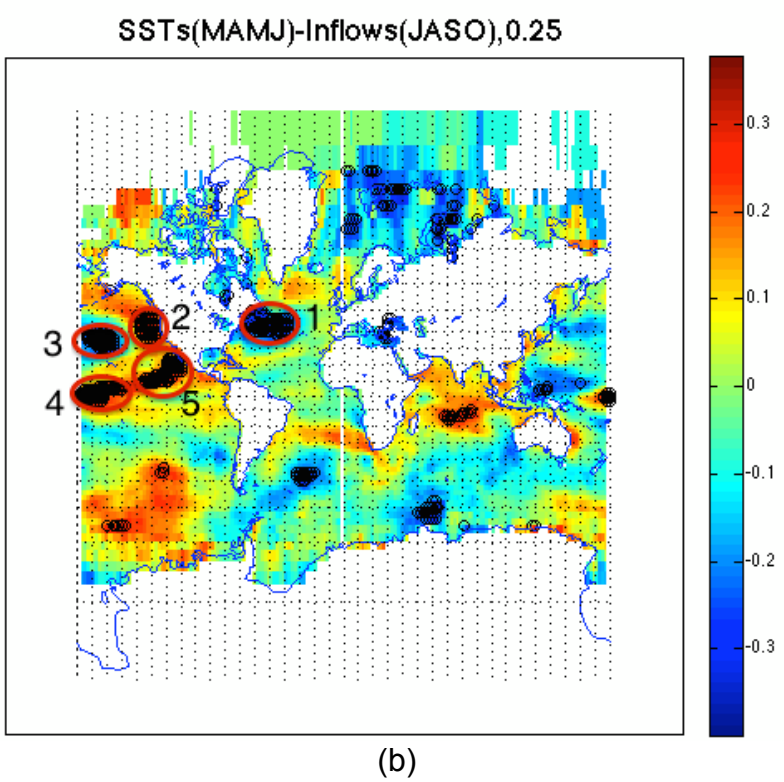

(b)

Figure 5: SST regions selected as predictor variables for MAMJ (a) and JASO (b) inflow forecasts. Statistically significant grid points are circled black and regions used in the study are outlined in red.

Spectral analysis is subsequently performed on the SST regions to understand if the periodicity coincides with any of the aforementioned indices (e.g. Nino 3.4, PDO, etc.) Spectral analysis applies a Fourier transform to decompose a noisy data signal from the time domain to the spectral domain. Cross spectral analysis reveals shared frequencies present in two time series (Rasmusson et al., 1981). Applying cross spectral analysis with the equatorial SST region identified (region 4 in Figure 5a) and the Nino 3.4 index, a large peak in the cross spectrum is visible in the range of 0.01 to 0.04 cycles per month, which aligns with the 3-7 year period associated with ENSO (Figure 6). The remaining SST regions did not share this power in the cross spectrum in this frequency range; however, they did

have statistically significant power in lower frequencies, possibly associated with PDO.

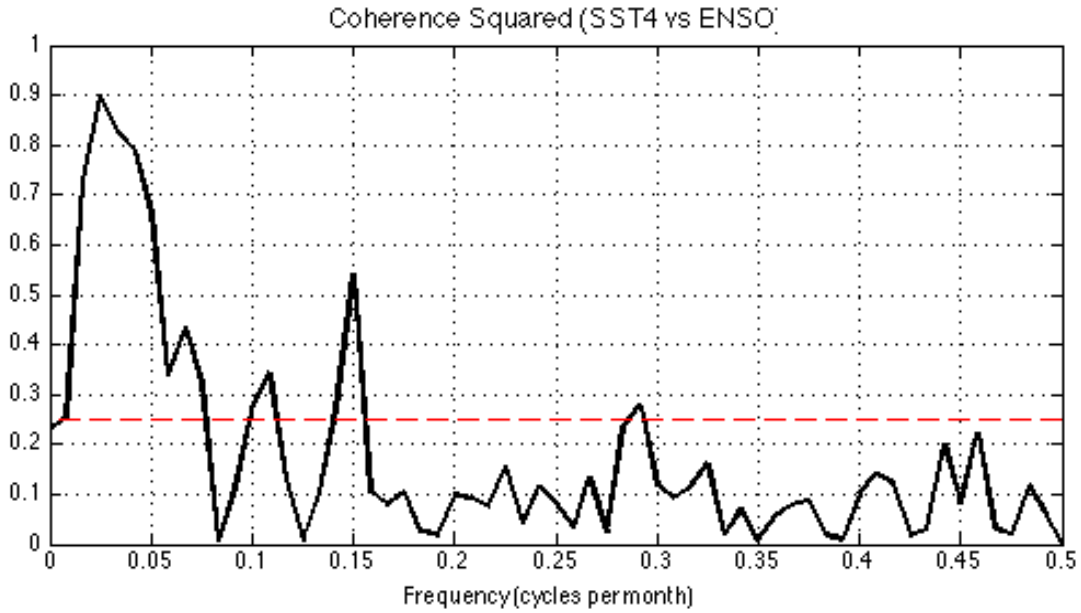

Figure 6: **Cross spectral analysis of SST Region 4 from Figure 3 and Nino 3.4 Index**

2.2.2.3 Sea Level Pressures

Due to the short-lived nature of sea level pressure systems, SLPs from only two months prior to the inflow season of interest are evaluated as potential predictors. Both January and February SLPs independently produce similar spatial patterns of statistically significant correlation with MAMJ inflows: predominantly one large region over the equatorial Pacific Ocean (Figure 7a). Similarly to SST regions, SLP regions were selected based on proximity to Texas. SLP grids from both months are retained and averaged for evaluation as a predictor. The months of May and June show two highly correlated regions in the Atlantic Ocean (Figure 7b) and are retained as possible JASO inflow predictors.

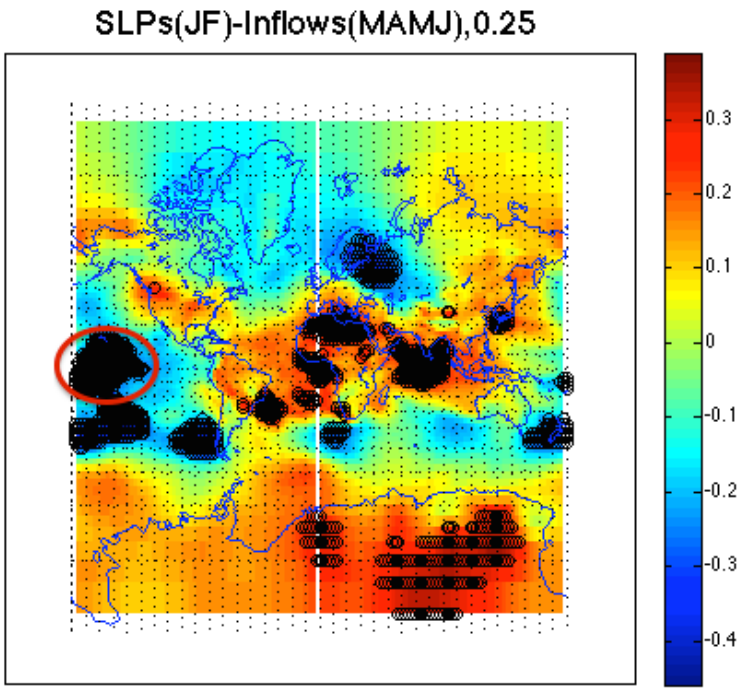

(a)

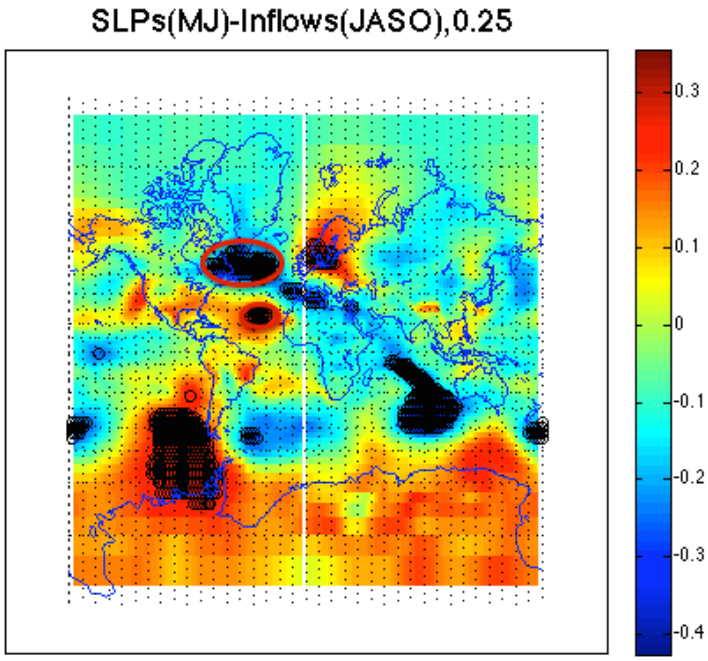

(b)

Figure 7: Statistically significant SLP regions chosen as predictors for MAMJ inflow forecast (7a) and JASO inflow forecast (7b)

Global predictor variables were selected based on correlation with total aggregate (TOT) inflows, not specifically for inflows into Buchanan (BUC) and inflows downstream of Lake Buchanan (DSBUC) independently (where TOT = BUC + DSBUC). It was assumed that global climate drivers would affect these adjacent sub-basins in a similar manner. While choosing SST and SLP regions of high correlation specific to each sub-basin may increase predictive skill modestly, it appears unjustified.

2.2.3 Local Predictors

2.2.3.1 Soil Moisture

Previous studies also have demonstrated that reduced soil moisture can prolong or amplify North American summertime droughts (Oglesby & Erickson, 1989; Seager et al., 2005). Anomalously low precipitation during winter and early spring months can lead to cumulative soil moisture deficits and reduced evapotranspiration, which leads to increased sensible heating and increased surface temperatures (Fernando et al., 2015). Hoerling et al. (2012) found that antecedent precipitation deficits and resulting dry soils was the principal physical process contributing to the extreme heat wave and drought in Texas during the summer of 2011. Texas has also been identified as a location where soil moisture can potentially increase the predictability of summer season precipitation (Koster et al., 2004). Soil moisture observations are not as readily available as other hydro-meteorological variables, particularly at the temporal and spatial coverage desired, thus modeled outputs are considered. Here, the

North American Land Data Assimilation System (NLDAS) land surface-model is selected (available 1979-present), simulating overall changes in soil moisture content in Texas (Sullivan & Maidment, 2012). Of particular interest is soil moisture in the top layer (0-10 cm.) February soil moisture averaged across the basin correlates at 0.53 with MAMJ inflows, a potentially strong prospective predictor. Soil moisture for June averaged across the basin only correlates at 0.18 with JASO inflows.

2.2.3.2 CFSv2 Precipitation Forecast

Finally, precipitation predictions from NOAA's Climate Forecast System Version 2 (CFSv2) dynamical model at 1°x1° for 1982-2010 (Saha et. al., 2013) are also retained as potential inflow predictors. Predictions of total precipitation issued at the beginning of February and June for the following four months (MAMJ and JASO) averaged across the basin and over all model realizations are used. CFSv2 precipitation forecasts correlate at 0.49 for MAMJ and 0.18 for JASO over 1982-2010.

2.3 Model Development

The following section presents the formulation of the ARMA portion of the hybrid model followed by methods for coupling the output with exogenous predictor variables in a principal component regression model.

2.3.1 Autoregressive Moving Average (ARMA) Model

Persistence in reservoir inflows has been illustrated as a skillful predictor, particularly across the spring (AMJ) and winter (OND) seasons (i.e. Wei & Watkins 2011). To capture this persistent feature, and due to the high autocorrelation present in the data, a univariate autoregressive model is selected. ARMA models have been recommended specifically for natural inflow systems with large storage capacity, low variability, and long response lags to precipitation events (Wang 2006). An ARMA(p,q) model uses the previous p values in the time series and the previous q white noise error terms. For hydrological purposes, low orders of p and q are typically selected for ARMA models (Wang & Salas, 1991). An ARMA(p,q) process can be modeled as

$$x_t = \varphi_1 x_{t-1} + \varphi_2 x_{t-2} + \ldots + \varphi_p x_{t-p} + \varepsilon_t + \theta_1 \varepsilon_{t-1} + \ldots + \theta_q \varepsilon_{t-q}. \quad (1)$$

where ε_t is a white noise error term which is normally distributed with a mean of zero. θ_q and φ_p are the coefficients on the lagged time-series values. Order selection of p and q is performed using Akaike information criterion (AIC; Akaike 1973) .

$$AIC(p,q) = \log(\sigma_\varepsilon^2) + 2(p+q)/N \quad (2)$$

where σ_ε^2 is the maximum likelihood estimate of the residual variance and N is the sample size. AIC seeks to maximize goodness of fit of the model while minimizing model complexity. A minimum AIC value is preferred.

Lag 1 autocorrelations for monthly inflow data are highest in March with a correlation of near 0.75 and correlations for January-July are all statistically significant, which is indicative of stronger persistence during these months (Figure 8).

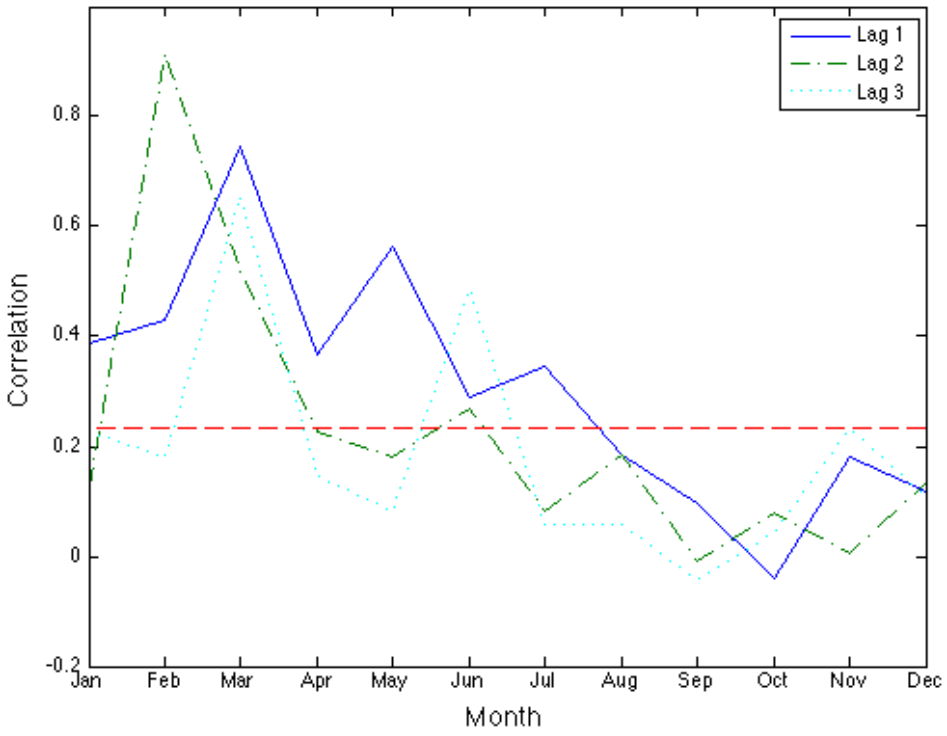

Figure 8: Monthly autocorrelation plot of Highland Lakes aggregate inflow data for lags 1-3 reveals statistically significant autocorrelation ($\alpha = 0.05$) for spring and summer months. Red dashed line is indicative of statistically significant correlation at the 95% confidence level.

As is common in hydrologic analyses, seasonal inflows are first transformed with the natural logarithm to approximate normality. To remove seasonality in the mean and variance, the inflow series was deseasonalized by subtracting seasonal means and dividing by seasonal standard deviations (Salas et al., 1993) (Figure 9).

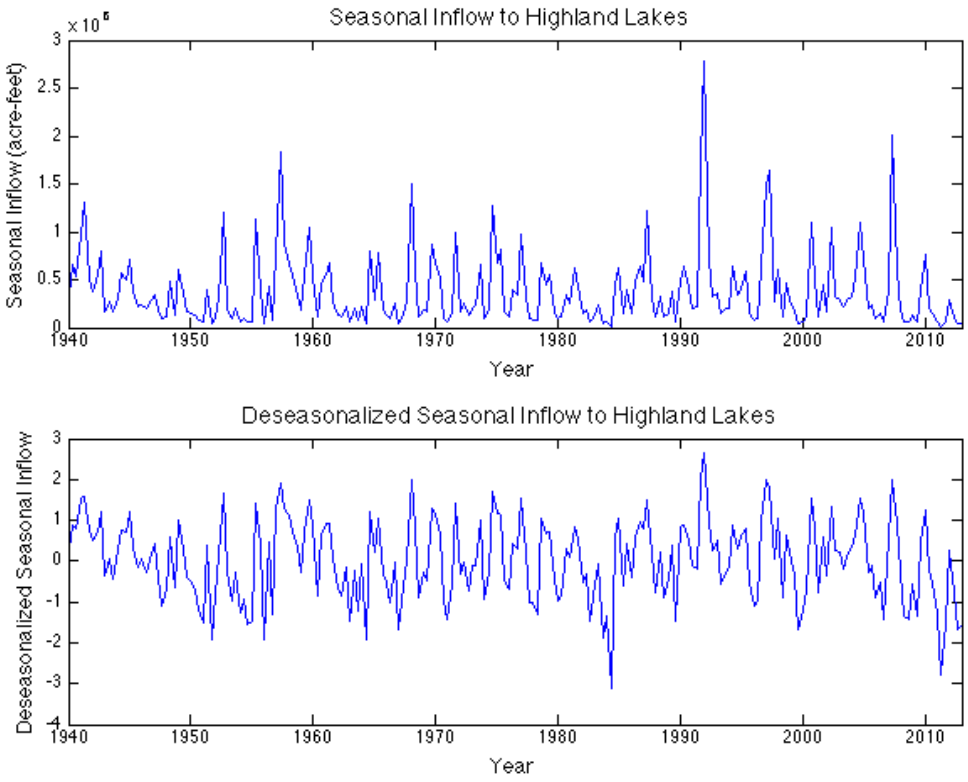

Figure 9: Observed inflow data (top) and deseasonalized inflow data (bottom)

Initial model identification is performed by examining plots of the autocorrelation function (Figure 10) and the partial autocorrelation function (Figure 11). The inflow time series is determined to be stationary using the Kwiatowski-Phillips-Schmidt-Shin (KPSS) test (Kwiatowski et al., 1992).

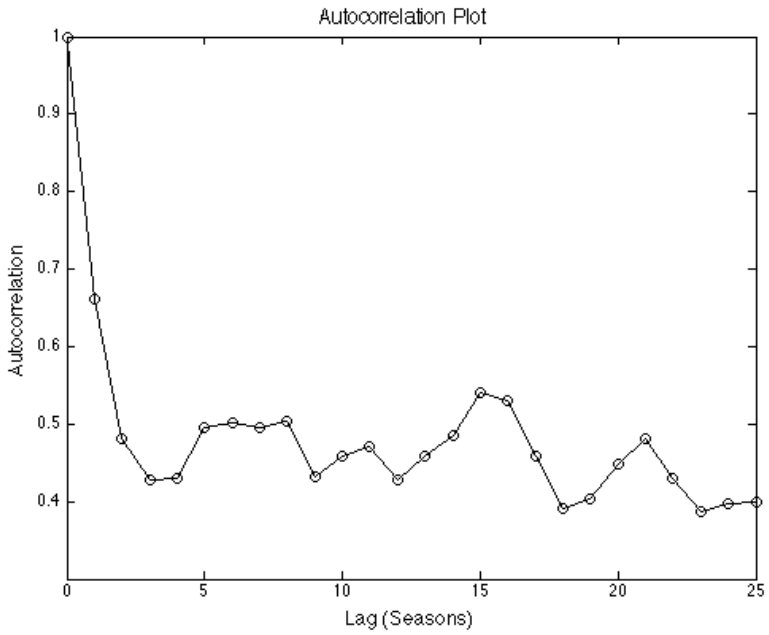

Figure 10: Autocorrelation plot of seasonal inflow data

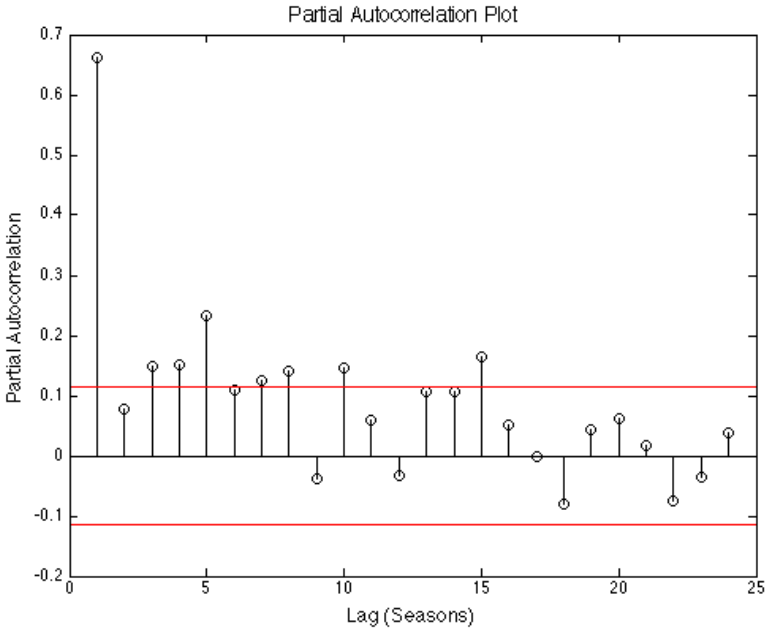

Figure 11: Partial autocorrelation plot of seasonal inflow data. Red lines on partial autocorrelation plot indicate statistically significant autocorrelation.

Individual ARMA models are created for each inflow time series: TOT, BUC, and DSBUC. Models with p and q vales of ARMA(3,2), ARMA(1,2), and ARMA(3,2) are selected, respectively, based on minimum values of AIC. Predictions for ARMA models are made at the termination of the season preceding the season of interest (i.e. end of February for MAMJ inflows). Correlations for the TOT and DSBUC ARMA models across all seasons (R=0.50 and R=0.51, respectively) indicate moderate predictive skill. TOT and DSBUC have higher correlation for the NDJF season due to more persistent low inflows during these months (Table 1). Correlation for the BUC model across all seasons (R=0.32) is lower than TOT and DSBUC but still statistically significant at the 0.05 significance level.

Table 1: Pearson correlation table for ARMA models

Season	TOT	BUC	DSBUC
ALL	0.50	0.32	0.51
MAMJ	0.49	0.39	0.53
JASO	0.38	0.25	0.38
NDJF	0.60	0.32	0.61

Other ARMA-type models were also evaluated, including an autoregressive integrated moving average (ARIMA) model, a periodic autoregressive (PAR) model, and a hydrologic persistence model. However, none demonstrate significant improvement over the ARMA approach.

2.3.2 Principal Component Analysis (PCA)

Many of the potential predictors identified in Section 3 exhibit collinearity, which may artificially increase performance metrics and give a false sense of the true

predictive skill. One commonly used method to decompose sets of data into orthogonal and uncorrelated time series eliminating multicollinearity, is PCA. PCA applies a linear transformation with the following mathematical formulation:

$$[PC] = [E][X] \quad (3)$$

where PC is a matrix containing vectors of principal components, E is a matrix containing eigenvectors, and X is a matrix containing the time-series of normalized predictor variables. The eigenvectors are selected such that the principal components (PCs) are in order of the percentage of total variation explained (e.g. Figure 12).

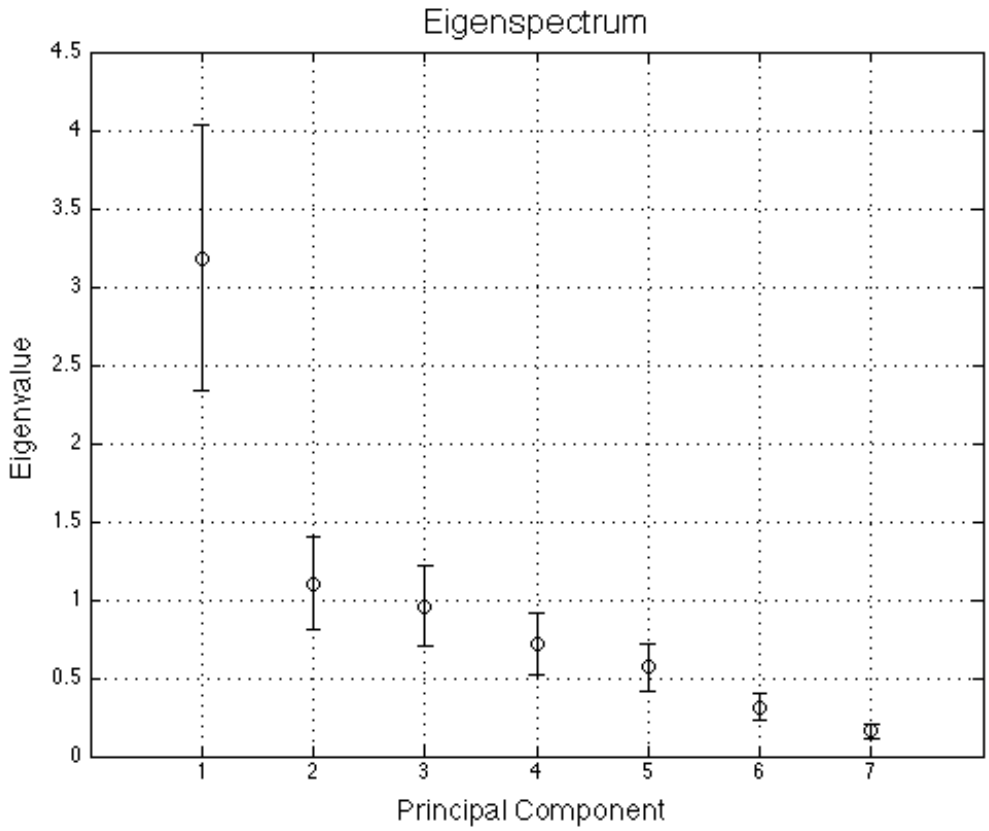

Figure 12: Eigenspectrum of MAMJ inflow forecast model using ARMA, soil moisture, CFSv2, and 4 SST regions as predictors. In this example, one principal component is retained based on North's rule of thumb.

The PCs capture the dominant temporal patterns present amongst the predictors. PCA produces *n* PCs for *n* predictors, however the first several PCs typically capture a majority of variability expressed by the original predictor variables. One simple method used to determine the number of PCs to retain is North's rule of thumb, which examines the sampling error between neighboring eigenvalues (North et. al., 1982). PCA offers a way to simplify a suite of predictors down to a minimal number of PCs. For a more detailed description of PCA, see Wilks (2011).

Since model performance metrics will be evaluated based on a hindcast, final PCs are constructed using a drop-one cross-validation technique for which one time step of all the predictor values is held out and the remaining data is used to generate a prediction. PCA is performed on the *n-1* variables and the corresponding eigenvalues are multiplied by the dropped data to reconstruct the predictor PCs. Each year of data was dropped individually (Stone 1978).

2.3.3 Multiple Linear and Logistic Regression Model

Both multiple linear regression (MLR) and multiple logistic regression (MLogR) models are assessed for their ability to predict reservoir inflow. MLRs fit a linear equation to two or more explanatory variables and a response variable.

$$y = \beta_0 + \beta_1 x_1 + \cdots + \beta_n x_n + \in \quad (4)$$

where y is the response variable, β_0 is a constant, $\beta_1 \ldots \beta_n$ are coefficients, $x_1 \ldots x_n$ are the predictor variables, and $\in$ is the error term. The coefficients are

determined using the least squares method, which minimizes the sum of squared errors.

MLogRs are used to discover relationships between a set of predictor variables and a set of discrete response variables. The response variable adopted here is categorical with three possibilities: above normal, near normal, and below normal inflows. These categories are defined as the upper 20th percentile, middle 60th percentile, and lower 20th percentile of the inflow data to represent wet, normal, and dry conditions, respectively, in order to more effectively capture extreme events. The MLogR model predicts the probability of inflow in each of category; there is no error term associated with the model as is the case with MLR. The simplest form of a logistic regression model involves two categories with probabilities *p* and *1-p*. A logistic model in linear form is:

$$\log(p/(1-p)) = \boldsymbol{\beta}_0 + \boldsymbol{\beta}_1 x_1 + \ldots + \boldsymbol{\beta}_n x_n + \in \quad (5)$$

with the $\boldsymbol{\beta}$ terms estimated using maximum likelihood theory and log(p/(1-p)) defined as logit(p). In this study, since the response variable has more than two categories, it is necessary to develop two logistic regression models for the three categorical responses. One category is selected as the baseline and the other categories are compared to it. Further details are available in Wei & Watkins (2011).

2.3.4 Model Performance Metrics

The hybrid autoregressive-principal component regression model proposed in this study incorporates the output of the ARMA models (endogenous predictor) with exogenous predictors, all transformed through PCA, as predictors in the regression models. To better understand the contributions of each potential predictor and groupings, and potentially maximize predictive skill, various subsets of predictors are assembled and subjected to PCA, and subsequently incorporated into MLR and MLogR models. When performing PCA, a common time period between all variables must be chosen. Thus, model calibration is limited by the predictor variable with the shortest time series.

Model skill is evaluated based on several metrics: correlation, AIC, rank probability skill score (RPSS), and generalized cross-validation score (GCVS.) The ranked probability score (RPS) measures the accuracy of forecasts when there are more than two categories by evaluating the cumulative squared difference between forecast category probability and observed category probability:

$$RPS = \frac{1}{K-1}\sum_{m=1}^{K}[(\sum_{k=1}^{m} f_k) - (\sum_{k=1}^{m} o_K)]^2 \quad (6)$$

where K is the number of forecast categories (3 in this case), f_k is the forecast probability for the given category, and o_K is 1 or 0 (o_K= 1 if the kth category contains the observed inflow, otherwise 0.) Values of RPS range from 0 to 1 with a perfect prediction having a value of 0 (Wei & Watkins 2011). RPSS measures

the relative improvement of a prediction over using climatology (probabilities of 20%, 60%, and 20% for below normal, near normal, and above normal inflows, respectively, as adopted here).

$$RPSS = 1 - \frac{RPS}{RPS_{climatology}} \quad (7)$$

Non-negative RPSS indicates an improvement in predictive skill when using the forecast as opposed to climatology. An RPSS of 1 indicates a perfect prediction.

The equation for GCV is as follows:

$$GCVS = \frac{\sum_{t=1}^{N} \frac{e_t^2}{N}}{(1-\frac{m}{N})^2} \quad (8)$$

where e_t is the model residual, N is the total number of data points, and m is the number of regression variables. Similar to AIC, a minimum value of GCV indicates a model that strikes a balance between high goodness of fit and low complexity (i.e. parsimony). GCV has been used in similar studies to select the best subset of predictor variables (Block & Rajagopalan, 2009; Regonda et. al., 2006).

2.4 Hybrid Model Results

In addition to discovering the optimal combination of predictors to maximize model skill, one intended outcome in this study is to better understand predictive skill of local (soil moisture, CFSv2 precipitation) versus global (SST, SLP, large-scale indices) variables. Predictors are thus evaluated individually, with

predictors from the same category (global and local), and in combinations of global and local predictors for BUC, DSBUC, and TOT for the MAMJ and JASO inflow seasons (Tables 2 & 3).

Table 2: Performance Metrics for selected combinations of predictors for total aggregate MAMJ inflows.

Predictors	R	GCVS	MLR RPSS	MLogR RPSS	Start yr.	End yr.
ARMA+SM	0.61	8.76	0.56	0.60	1982	2013
ARMA+CFSv2	0.50	10.42	0.54	0.62	1982	2010
ARMA+Local(SM,CFSv2)	0.66	7.75	0.65	0.70	1982	2010
ARMA+SLP	0.52	11.10	0.51	0.53	1951	2013
ARMA+SST(all 4 regions)	0.52	10.58	0.51	0.53	1941	2013
ARMA+N3.4	0.43	12.37	0.50	0.52	1951	2013
ARMA+ Global(SST,SLP, N3.4)	0.52	11.06	0.49	0.53	1951	2013
ARMA+Local(SM,CFSv2)+ Global(SST,SLP, N3.4)	0.60	8.91	0.61	0.65	1982	2010
ARMA+Local(SM,CFSv2)+SST4	**0.70**	**7.04**	**0.67**	**0.73**	**1982**	**2010**

Table 3: Performance Metrics for selected combinations of predictors for total aggregate JASO inflows.

Predictors	R	GCVS	MLR RPSS	MLogR RPSS	Start yr.	End yr.
ARMA+SM	0.24	15.96	0.51	0.55	1979	2013
ARMA+CFSv2	0.39	12.61	0.48	0.54	1982	2010
ARMA+Local(SM,CFSv2)	0.37	11.93	0.48	0.52	1982	2010
ARMA+SLP(2 regions)	0.50	11.86	0.52	0.54	1950	2013
ARMA+SST(all 5 regions)	0.52	11.20	0.53	0.59	1941	2013
ARMA+N3.4	0.29	14.04	0.47	0.50	1950	2013
ARMA+ Global(SST,SLP, N3.4)	0.51	11.37	0.52	0.59	1950	2013
ARMA+Local(SM,CFSv2)+ Global(SST,SLP, N3.4)	0.49	11.01	0.54	0.63	1982	2010
ARMA+ SM+SST	**0.64**	**9.78**	**0.56**	**0.64**	**1979**	**2013**
ARMA+ CFSv2+SST+SLP	**0.63**	**9.42**	**0.55**	**0.65**	**1982**	**2010**
ARMA+SST+SLP	**0.58**	**10.20**	**0.56**	**0.65**	**1948**	**2013**

Local predictors contribute more predictive skill for the MAMJ season than global predictors (e.g. correlations of ~0.60 vs ~0.51.) The opposite appears to be true for the JASO season, where models with only ARMA and local predictors illustrate much lower correlation than those with only global predictors (correlations of ~0.33 vs ~0.46) The physical mechanisms responsible for this shift are still under investigation at this time. Soil moisture is a skillful predictor for MAMJ inflows (r = 0.61) but not for JASO inflows (r = 0.24), where it is the weakest predictor. SSTs are robust predictors for both inflow seasons (r = 0.52 and r = 0.52)

Overall, models performed best with a combination of ARMA, local and global predictors (Tables 2 & 3). Considering all performance metrics outlined in Section 4, the strongest model for MAMJ inflows included ARMA, soil moisture, CFSv2 precipitation forecasts, and SST region 4 as predictors. Categorical results for this model are seen in Figure 13. This combination had the best results across all performance metrics (Table 2.) Using other SST regions provided similar, although slightly inferior, outcomes.

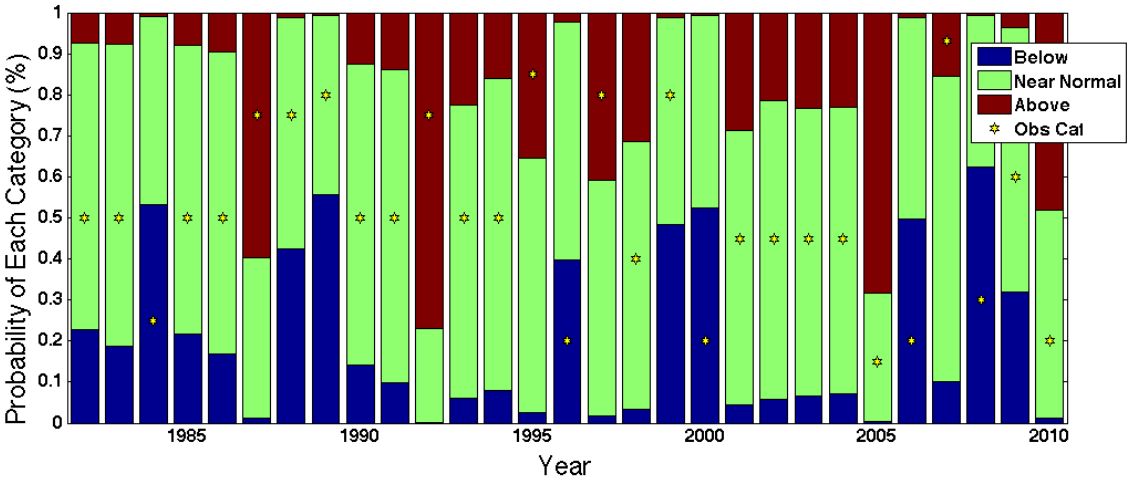

Figure 13: Categorical results of the same model as Figure 12 with observed category denoted by a star. Each color (category) represents the expected probability of the observation falling in that category.

JASO inflow forecast models did not have one dominant predictor combination that performed best across all metrics. Three combinations are approximately on par, including 1) soil moisture and SSTs, 2) CFSv2 and SSTs and SLPs, and 3) SSTs and SLPs (Table 3.) Categorical results for the second of the above combinations are presented in Figure 14.

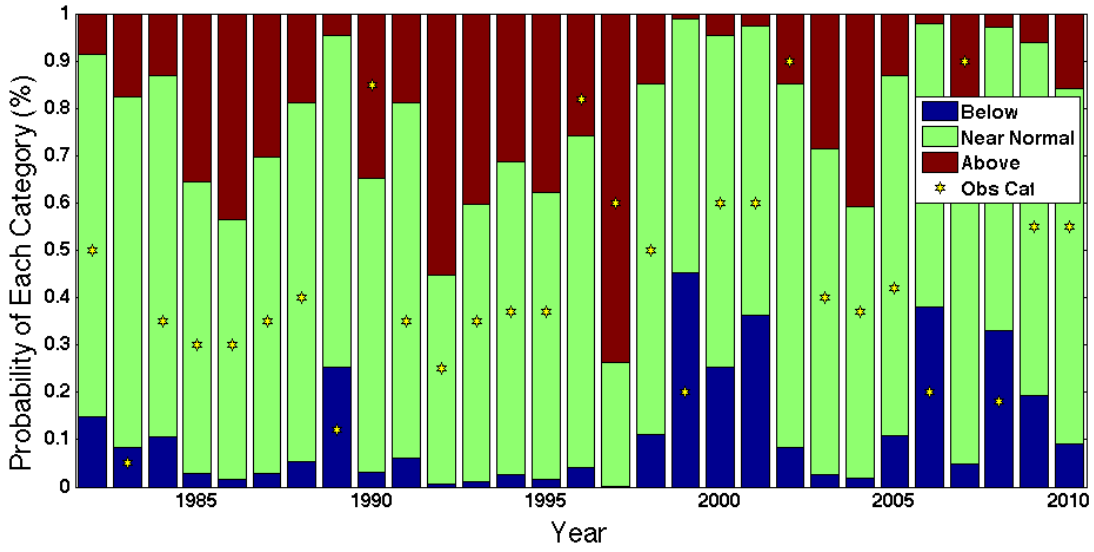

Figure 14: Categorical results for JASO inflow predictions

Hindcasts of MAMJ inflows from 1982-2010 tend to show strong agreement with observations using both the MLR and MLogR model approaches. On average, hindcasts of MAMJ inflows illustrate higher predictive skill than hindcasts of JASO inflows, agreeing qualitatively with Wei & Watkins (2011) (Tables 2 & 3), however the hybrid autoregressive-principal component regression method demonstrated significant quantitative improvement compared to their results (RPSS values of 0.17 and 0.148 for April-June and July-September seasons, respectively). MLogR models tend to produce higher values of RPSS than the MLR models, likely due to the categorical nature built into these types of models. Both MLR and MLogR models assume linear relationships; other nonlinear techniques may help to elucidate the complex interactions present in atmospheric-oceanic dynamics and hydrological processes.

BUC predicted inflow performance measures are inferior to DSBUC and TOT for both MAMJ and JASO seasons. The values for GCVS are an order of magnitude larger and correlations tend to be smaller. One possible reason is the manner in which the inflow data was adjusted to account for the introduction of the OH-Ivie reservoir in 1990, resulting in several months with no flow, skewing the time-series.

The MAMJ inflow prediction model performs poorly in 1984 (Figure 15). The model predicted the correct category (below normal) however it was unable to capture the severity of the drought for that year.

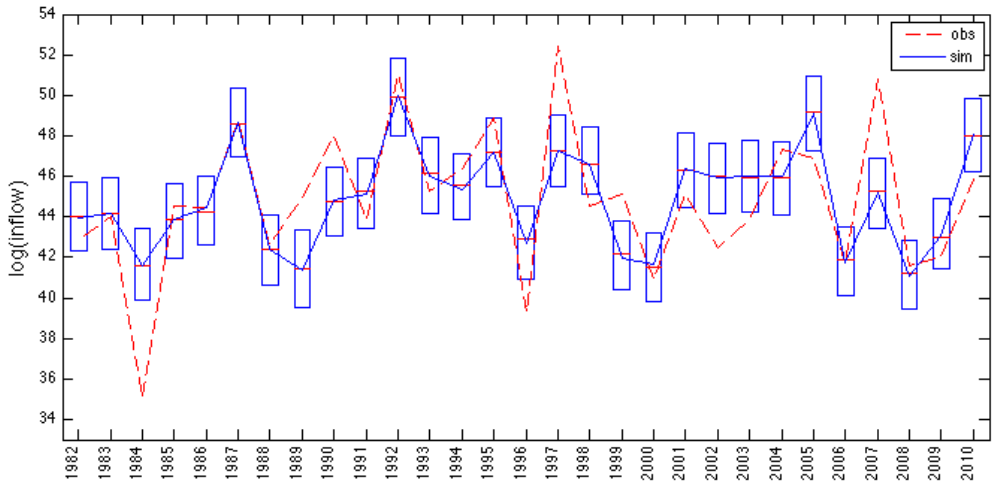

Figure 15: Model results of total aggregate MAMJ inflows using ARMA, soil moisture, CFSv2, and SST as predictors in a PCR model. The top and bottom of the box plots correspond to 25th and 75th percentiles of the simulations.

Some preliminary investigation revealed that soil moisture for the preceding season was anomalously high when compared to other years with below normal inflows, leading to an over-prediction of inflows. SST anomaly patterns for 1984 also differ compared to other dry years; SST anomalies along the equator were not as low and an unusually warm region of water was located off the west coast of North America which may have increased evaporation in this area and brought more moisture across the southern United States.

It is important to note that not all predictor combinations share a common observational period, resulting in models being trained on a dissimilar number of years (Tables 2 & 3). CFSv2 and soil moisture are the limiting predictors (29 and 34 years, respectively), and although combinations with these predictors require a higher correlation value to be statistically significant, direct comparison with combinations having longer observational records requires caution.

CHAPTER 3: Reservoir Operation Simulation

This chapter evaluates how linking a reservoir systems model with predictive information, specifically a reservoir inflow forecast, can inform water allocations objectively and dynamically by season.

3.1 Highland Lakes Simulation Data

3.1.1 Reservoir Inflows

Monthly reservoir inflow data to the Highland Lakes (1940-2013) was provided courtesy of the LCRA. Reservoir inflows to the Highland Lakes are calculated based on four USGS streamflow gages located on the Colorado River, Llano River, Sandy Creek, and Pedernales River (Figure 1). The four gages are not located directly on the Highland Lakes; a runoff factor as provided by the LCRA is applied to each of the measured streamflows to account for water inflow downstream of the gages. Average monthly inflows are highest in the month of May with a second peak in inflows in October (Figure 4), although there is significant interannual variability. To match the decision points for the LCRA and the crop seasons, monthly inflows are summed into three seasons: March-June (MAMJ), July-October (JASO) and November-February (NDJF).

Historical Reservoir Levels

Historical lake levels for Lake Travis and Lake Buchanan were obtained from the LCRA website (http://www.lcra.org/water/river-and-weather/pages/historical-lake-levels.aspx). Average monthly levels were used in conjunction with elevation area capacity curves from the Texas Water Development Board

(http://www.twdb.texas.gov/hydro_survey/travis/2008-07/Travis2008_FinalReport.pdf ; http://www.twdb.texas.gov/hydro_survey/Buchanan/2006-04/Buchanan2006_FinalReport.pdf) to obtain combined storage levels. Historical combined storage levels can be seen in Figure 2.

3.1.2 Firm Demands

Total annual firm water demands are taken to be constant for this simulation as 150,000 acre-feet, the average firm water diversion for the time period 2009-2014 (LCRA, 2014). This includes diversions for municipal use (city of Austin, TX), industrial use (power plants) and other uses (recreation, firm irrigation).

Firm demands change over the course of the year with highest demand occurring during the summer months. The seasonal firm demands are calculated to reflect the varying requirements. Monthly fractions of annual firm demand from Watkins, 1999 were summed for each season and multiplied by the annual total of 150,000 acre-feet. Resulting seasonal firm demands are 47,600 acre-feet, 62,900 acre-feet, and 39,500 acre-feet for MAMJ, JASO, and NDJF seasons, respectively (Table 4).

Table 4: Constant water allocations for reservoir simulation

(acre-feet)	MAMJ (First crop season)	JASO (Ratoon crop season)	NDJF	Annual Total
Firm	47,600	62,900	39,500	150,000
Environmental	15,380	11,040	7,020	33,440
Garwood Irrigation	25,500	9,500	0	35,000

In addition to the firm demands, the LCRA also maintains a contract with Garwood irrigation operations in accordance with the Garwood Purchase Agreement. Although this water is viewed as a portion of the Interruptible Water Supply, the newest revision of the WMP states 35,000 acre-feet is allocated to Garwood every year. For the sake of simplicity, the Garwood irrigation diversion is viewed as a firm demand as it does not change from year to year. The annual Garwood demand is split between the two crop seasons, MAMJ and JASO, based on the split of maximum interruptible water allocations for the two crop seasons from the WMP; 73% of the total Garwood allocations (25,500 acre-feet) for MAMJ and 27% of Garwood allocations (9,500 acre-feet) for JASO. (Table 4).

3.1.3 Environmental Demands

The LCRA also manages water for environmental purposes. Freshwater from the Highland Lakes is critical for maintaining an appropriate aquatic environment for many species of flora and fauna present in the LCRB. The LCRA has committed to releasing 33,440 acre-feet of water from the Highland Lakes to maintain an instream flow in the Colorado River and for the delicate estuary environment in Matagorda Bay. As with firm demands, environmental flow requirements vary during the year with demand being maximal in the spring months. Monthly fractions of total environmental flow demand were acquired from the WMP and summed for each season. Total annual firm demands are constant for the simulation with seasonal totals of 15,380 acre-feet, 11,040 acre-feet, and 7,020 acre-feet, for MAMJ, JASO, and NDJF (Table 4).

3.1.4 Evaporation Data

Evaporation makes up a significant portion of the Highland Lakes water balance; therefore it is critical to correctly estimate totals to ensure accurate simulation results. Monthly pan evaporation data from 1954 to 2013 was obtained from the Texas Water Development Board (TWDB) website (http://midgewater.twdb.texas.gov/evaporation/quadrangle/710/evaporation-tabular.txt). Average annual evaporation is 4.36 feet with a standard deviation of 0.44 feet. Monthly lake surface evaporations were summed for each season (MAMJ, JASO and NDJF). Average evaporation is highest for the JASO season (μ = 1.98 ft) followed by MAMJ (μ = 1.57 ft) and NDJF (μ = 0.81 ft). Evaporation is a function of combined storage of Lake Travis and Lake Buchanan; higher values of combined storage yield a larger surface area and therefore more evaporated water. Elevation-Area-Capacity (EAC) tables for Lake Buchanan (http://www.waterdatafortexas.org/reservoirs/individual/buchanan/rating-curve/twdb/2006-03-01) and Lake Travis (http://www.waterdatafortexas.org/reservoirs/individual/travis/rating-curve/twdb/2008-07-01) were used to determine lake surface area based on average combined storage for each season.

3.1.5 Forecasted Inflow Simulations

A seasonal hybrid autoregressive-principal component regression model is developed for the LCRB for the two crop seasons. The model combines an autoregressive moving average (ARMA) model with various local (soil moisture, CFSv2 precipitation forecasts) and global (climate indices, sea surface

temperatures, sea level pressures) predictors in a principal component regression framework. Principal component analysis (PCA) is applied to the ARMA results and predictors selected based on performance metrics. PCA identifies the dominant modes of variability, or principal components, common to the selected time series. These principal components are then used as predictors. Forecasts are issued at the start of each crop season and are probabilistic in nature.

A combination of both local and global predictors provides strongest performance of the models. ARMA, sea surface temperatures, CFSv2 precipitation forecasts, and soil moisture were selected as final predictors for the MAMJ season (correlation = 0.70; RPSS = 0.73) (Figure 13). The JASO forecast model had lower predictive skill with a correlation of 0.63 and RPSS of 0.65 (Figure 14). ARMA, sea surface temperatures, sea level pressures, and CFSv2 precipitation forecasts were used as predictors for the second crop season. These models demonstrate a significant improvement over other inflow models previously developed for the model in Watkins, 2011, where forecasts for the April-June and July-September seasons had RPSS values of 0.17 and 0.15, respectively. The reservoir inflows predictions are ouput in a probabilistic manner to capture climate variability.

3.2 CONDITIONING RESERVOIR OPERATIONS ON PREDICTED INFLOWS

3.2.1 Simulation of Reservoir Operations

Water allocation decisions are set at the beginning of each season, with no intra-seasonal changes in allocation allowed. In determining these pre-season allocations, water managers must be able to account for inflows into reservoirs to anticipate future conditions. Traditionally, static historical averages are used to anticipate inflows for a given season. An inflow forecast may indicate a shift toward wetter or dryer conditions, allowing water managers to make different allocations than they may without such information. To better understand the value and implications of forecast and no-forecast approaches to allocation decisions, both are evaluated. Specifically, reservoir operations and water allocations for the Highland Lakes are compared under two conditions: a) Forecast: using inflow predictions from the principal component regression forecast and b) No-Forecast: using historical averages of inflows, referred to as climatology. For the sake of simplicity, the storage levels of both Lake Travis and Lake Buchanan are combined into a single pool supply. The beginning of the water year is taken as March with the first crop season (March-June) being season 1, the second crop season (July-October) being season 2, and the winter season (November-February) being season 3.

Both Forecast and No-Forecast simulations begin with a historical value for combined storage to match observed conditions for that given time period. This value of combined storage is used to simulate evaporation and uses forecasted

or average inflows to determine IWA through an objective function. The exact values of evaporation and inflows are not known at the time of issuing IWAs and thus averages and forecasts are used at the beginning of crop seasons. These values are later corrected with observations from that season in a water balance model, which uses the IWA along with observed values of inflows (IN) and evaporation (E) to calculate the combined storage level for the next time step, S_{t+1}. The procedure is repeated until the termination of the simulation (Figure 16).

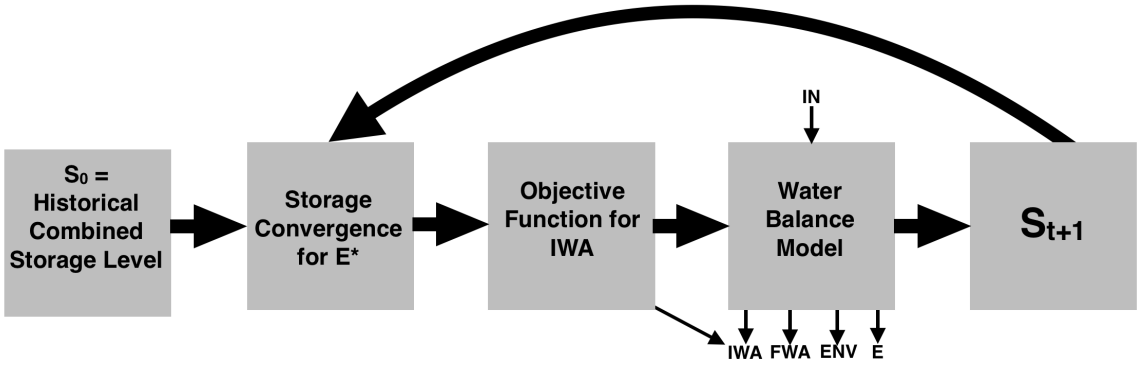

Figure 16: General procedure for reservoir operation simulation

The objective of the simulation is to determine non-Garwood IWAs, such that the probability of meeting an end of season storage target is greater than $(1-p_f)$, where p_f is the probability of failure (Equation 9). This is a similar approach to Sankarasubramanian et. al., 2009. Higher values of IWA are viewed as more beneficial to the interruptible water customers within the LCRB.

$$\text{Prob}(S_{t+1} > S_{target}) \geq (1-p_f) \quad (9)$$

S_{target} is set as 1.3 million acre-feet, or one of the criteria for meeting Extraordinary Drought conditions in the current WMP; p_f is evalauted at 5%, 25%, and 50% of the expected (forecast or climatology) inflow distribution.

3.2.2 Procedure for Storage Convergence

End-of-season storage and evaporation are codependent, requiring an iterative approach based on average seasonal storage S_{avg}. The procedure is as follows:

1) Set $S_{avg} = S_t$
2) Obtain surface area A_t of reservoirs from Elevation Area Capacity tables based on S_{avg}
3) Total estimated seasonal evaporation $E_t^* = A_t e_t^*$ where e_t is average seasonal evaporation rate from Texas Water Development Board
4) Calculate IWA_t based on look-ahead optimization
    a. For crop seasons (seasons 1 & 2), calculate end of season storage without IWA_t or inflows: $S^*_{t+1}=S_t-E_t-FWA_t-ENV_t$
    b. Select $IN_{fail,t}$, inflow from ESP at the chosen failure rate percentile (e.g. 5%).
    c. $IWA_t= S^*_{t+1}+ I_{fail,t} – CS_{min}$ where CS_{min} is minimum combined storage for the objective function (1.3 million acre-feet). Minimum IWA_t is 0 acre-feet.
5) Calculate final storage for period t: $S_{t+1}^* = S_t+IN_{fail,t}-E_t^*-IWA_t-ENV_t-FWA_t$ where ENV is environmental water demands and FWA is firm water allocation.
6) If $S_{t+1}^* > S_{max}$ (total storage capacity, or 2.01 million acre-feet), set S_{t+1} as 2.01 million acre-feet and record spill volume
7) Find the new average storage $S^*_{avg} = (S_t + S_{t+1})/2$

8) Set S_{avg} = S^*_{avg} and repeat steps 2-6 until S_{avg} and S^*_{avg} are within 1% of each other. The values of E_t and IWA_t are acceptable at this point.
9) Correct S_{t+1}* with observed inflows and evaporation rates for given time step to obtain $S_{t+1} = S_{t+1}^* + \Delta IN_t + \Delta E_t$

Tests indicate six iterations or less are sufficient for convergence.

A reservoir mass balance equation is applied at the end of each time step of the simulation using observations. (Equation 10)

$$S_{t+1} = S_t + IN_t - E_t - IWA_t - ENV_t - FWA_t \quad (10)$$

Where IN is observed inflow volume and E is observed evaporation volume.

3.2.3 Rules for IWA Allocation

The newest revision of the WMP has maximum values for IWA based on the existing water supply condition. The evaluation date is defined as the first day of each crop season, March 1 and July 1. The existing water supply condition is based on the following criteria:

1) Normal: Neither Less Severe drought nor Extraordinary Drought conditions were in effect for the period prior to the evaluation date and criteria for these two conditions are not met for the current period.
2) Less Severe Drought: On the evaluation date, combined storage is below 1.6 million acre-feet and cumulative inflows into the Highland Lakes for the preceding three months are less than 50,000 acre-feet OR combined storage is less than 1.4 million acre-feet on the evaluation date and

inflows to the Highland Lakes for the three months prior are at the 33rd percentile or below for that three month inflow period.

3) Extraordinary Drought: On the evaluation date, combined storage is less than 1.3 million acre-feet, the drought duration is more than 24 months, and criteria for the inflow intensity test are met (Figure 17). For drought duration, the beginning of the drought is defined as the last occasion on which combined storage is greater than 98% of total storage capacity (1.97 million acre-feet).

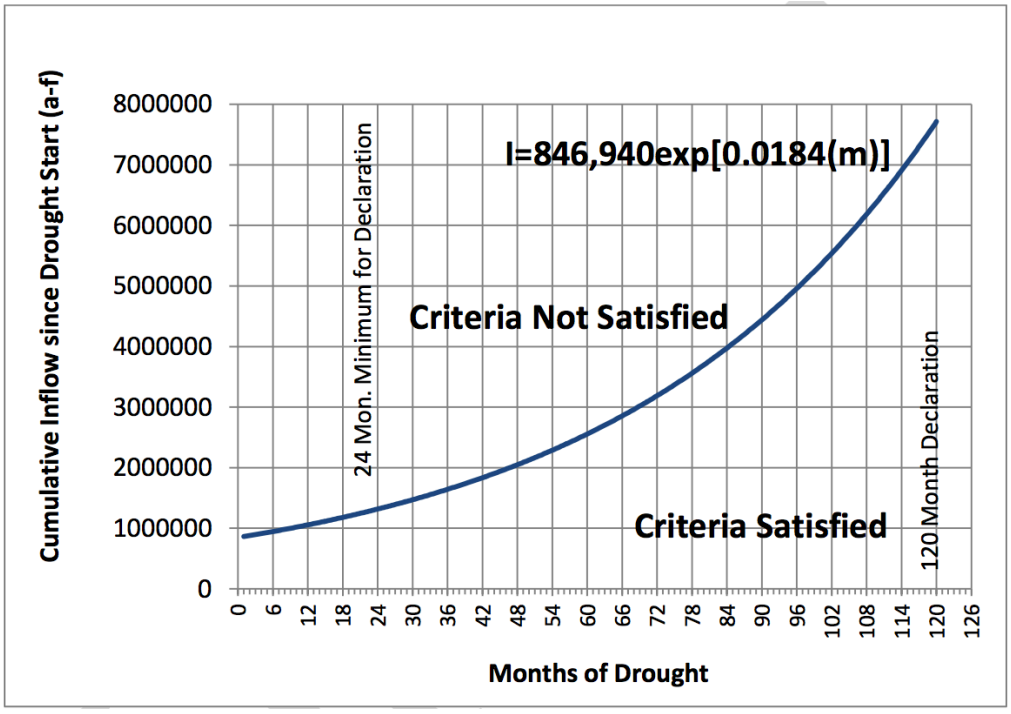

Figure 17: Drought intensity curve for determination of Extraordinary Drought (courtesy of LCRA)

The WMP also issues criteria for exiting drought conditions:

1) Less Severe Drought: To return to Normal condition from Less Severe condition, combined storage must surpass 1.6 million acre-feet for the

preceding season and neither of the criteria for Less Severe drought are met on the evaluation date OR combined storage is less than 1.4 million acre-feet and inflows for the previous three months surpass the 50th percentile of inflows for that time period.

2) Extraordinary Drought: Combined storage surpasses 1.3 million acre-feet for the season preceding the evaluation date and criteria for Extraordinary Drought are not met. If these criteria are met, then the water supply condition is set as Less Severe, unless criteria for exiting Less Severe drought are also met then water supply condition is set to Normal.

IWAs are strictly defined in the WMP based on current water supply conditions (Table 5). For Normal conditions, maximum IWAs are 202,000 acre-feet and 76,500 acre-feet for the first and second crop seasons, respectively. For Less Severe Drought, maximum IWAs are 155,000 and 55,000 acre-feet for the first and second crop seasons, respectively. No water is allocated for non-Garwood irrigation in an Extraordinary Drought.

Table 5: Maximum IWAs from WMP (acre-feet)

Drought Condition	First Crop Season	Second Crop Season
Normal	202,000	76,500
Less Severe	155,000	55,000
Extraordinary	0	0

The simulation is initiated with observations of combined storage from the end of water year 1981 and run for the 29 years of the forecast model (1982-2010). With three seasons per year, there are a total of 87 time steps or seasons. A failure

probability of 5% is used in the simulations in the following section and a sensitivity analysis of failure probabilities (5%, 25%, 50%) follows.

3.3 Reservoir Simulation Results

The following section presents results for the simulation with the forecast (Forecast) and without the forecast (No-Forecast). Reservoir simulations are evaluated for two IWA allocation modes:

1: Non-restricted: having no upper limit on the maximum IWAs allocated

2: Restricted: using the maximum IWAs prescribed in the WMP

3.3.1 Non-restricted IWA Simulation

The results for the non-restricted simulation help to elucidate the aggregated benefits of using a seasonal reservoir inflow forecast over long-term operations. This simulation is free running for the entire timespan without annual resets to match historically observed storage levels. Combined storage levels for simulations with the Forecast and with No-Forecast are presented in Figure 18. Combined storage patterns of Forecast and No-Forecast simulations yield similar storage patterns. Reliability in the simulation is measured as the percentage of seasons with combined storage above 1.3 million acre-feet. Using a forecast provides marginally increased reliability of 92.0% versus 90.8% with climatology.

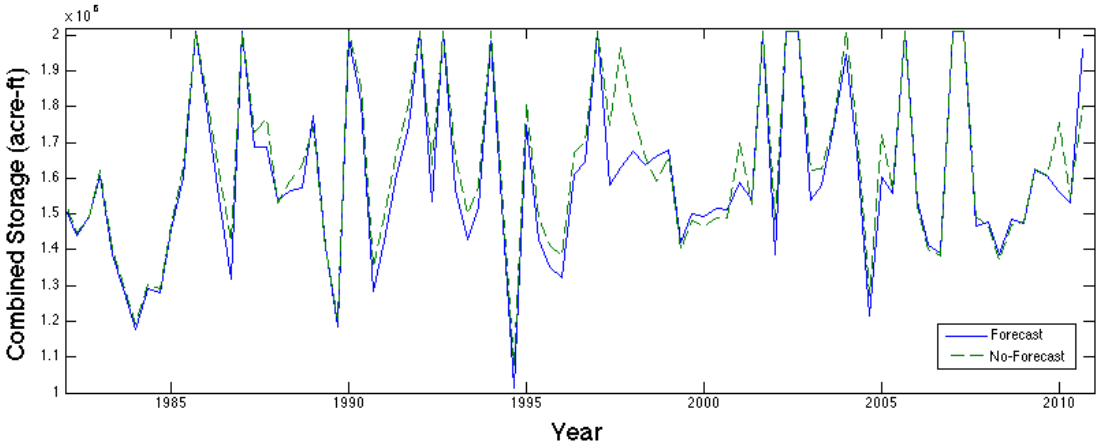

Figure 18: Combined Storage of reservoirs with non-restricted IWAs

IWAs with the Forecast simulation for both crop seasons demonstrate an increased range when compared to No-Forecast. (Figure 19) This is most visible on the positive end when using the forecast predicts wet conditions and more water is allocated. When dry conditions are forecasted and existing storage levels are low, both the Forecast and No-Forecast simulation runs allocate zero water towards IWAs. Mean values of IWA for both crop seasons are approximately 10% larger for the Forecast simulation (225,310 acre-feet vs 205,660 acre-feet). Under these conditions, the forecast benefit is greater allocations in anomalously wet seasons.

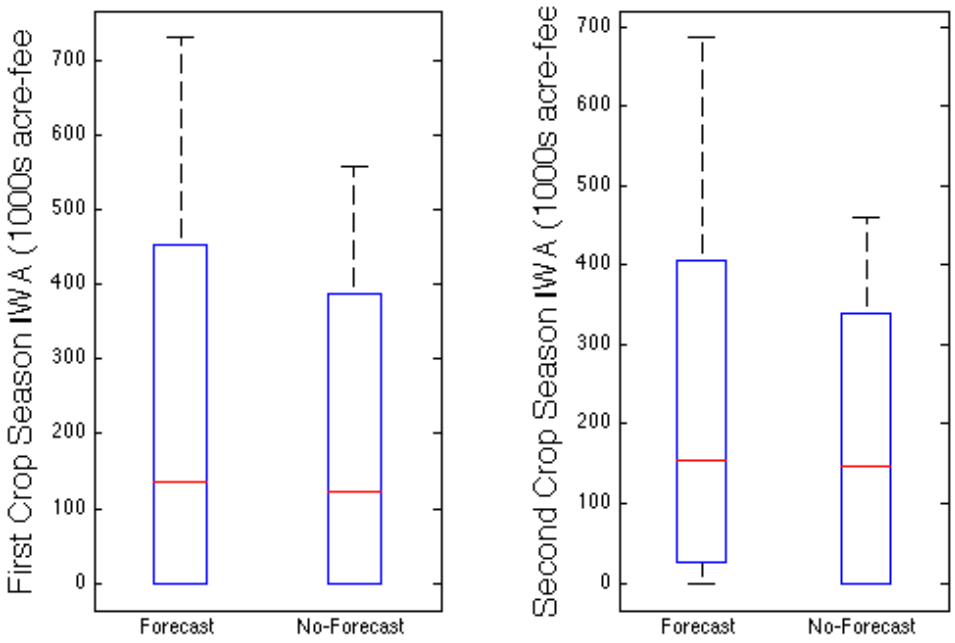

Figure 19: Boxplot of IWAs for first and second crop seasons for non-restricted IWA simulation

Isolating the six wettest and driest seasons in terms of inflows for both the first and second crop seasons within this simulation (approximately the upper and lower 20th percentiles) assists in highlighting how the forecast impacts decision-making during extreme events. Of the 6 driest first crop seasons within the simulation (1984, 1996, 2000, 2002, 2008, 2009), the Forecast and No-Forecast results have two seasons where 0 acre-feet was allocated towards IWA, two seasons where the Forecast has smaller IWA than No-Forecast, and two years where No-Forecast has smaller IWA than the forecast. The forecast simulation yields four seasons with lower IWA for the driest second crop seasons (1982, 1983, 1989, 1999, 2006, 2008). For the wettest seasons (1987, 1990, 1992, 1995, 1997, and 2007 for first crop season and 1987, 1990, 1996, 1997, 2002, and 2007 for the second crop season), both first and second seasons allocate

more water towards IWA for all but two instances. These allocations are reliant on existing storage levels and whether the forecast calls for less than or greater climatological inflows.

Overall, the forecast causes a higher variability in IWAs during the non-restricted simulations due to lower IWAs when dry conditions are forecasted and increased IWAs when wet conditions are forecasted. When the six seasons with the lowest inflows are analyzed within the long-term simulation, the forecast typically prescribes lower or similar IWAs for those seasons, leading to higher storage being maintained in the short term. For the six seasons with highest inflows, allocations are significantly higher with the forecast leading to less “wasted” water. As a result, the forecast yields storage levels that are more consistent and have a slightly lower variability than when not using the forecast. This is beneficial from the perspective of water managers as this allows for more reliable planning.

One area of significant improvement when using the forecast is in terms of spills. Spills occur any time the storage is greater that 2.01 million acre-feet. This excess water is released downstream with no benefit to water users. Minimizing the spill volume provides increased utility of this water, especially to interruptible water customers. When the forecast is implemented, spills occurr during 11 of the 87 seasons, compared to 13 when using climatology. Total spill volume over the entire 29-year duration of the Forecast simulation results is 7.75 million acre-feet compared to 8.41 million acre-feet with No-Forecast, allowing for 660,000 acre-feet of water to be used for more beneficial purposes. It is clear that by

implementing a forecast during times of anomalously high inflows (flooding), more water is allocated towards interruptible water allocations leading to a lower overall spill volume. Each time that a spill occurs for simulations, it serves as a "reset" where storages for both simulations converge and are both set at the maximum capacity of the reservoirs.

3.3.2 Restricted IWA Simulation

The maximum IWAs prescribed by the WMP are significantly lower than the allocations based on reliability of meeting end of season storage. Therefore, when the restrictions are applied, IWAs are nearly always set at maximum values, which are dependent on season and water supply condition. There are four seasons where maximum IWAs are not used with the Forecast simulation and five seasons with No-Forecast. As a result, combined storage of both simulations is nearly identical. One benefit of restricted IWAs is that both simulations have a reliability of 100% for maintaining storage above 1.3 million acre-feet. It is clear that with the restricted IWAs, the average combined storage levels are higher than non-restricted (1.87 million acre-feet vs 1.62 million acre-feet, respectively). However, this leads to a significantly larger total spill volume of 17.9 million acre-feet for both No-Forecast and Forecast simulation runs. Thus the forecast is of limited value with current restrictions on IWA, however the non-restricted approach could eventually promote an allocation system without maximum IWAs.

The conservative values of maximum IWAs were issued in response to the most recent drought to avoid depleting water supplies if a drought of similar magnitude

were to occur in the near future. These restricted IWAs are also low when compared to historical IWAs. With restrictions set at the current levels and using a reliability-based allocation, the benefits of using a forecast are being forfeited based on simulation results. Forecasts, however, can be used to set up restrictions during below-normal inflow years (Golembesky et. al., 2009). This would increase the utility of the forecast in reservoir management.

3.3.3 Extreme Year Simulation Runs

To understand the short-term impacts of implementing a forecast into reservoir operations during extreme events, simulations are also run with initial conditions set to match observed storage conditions during these years. These simulations are run without IWA restrictions. Two anomalously wet seasons and two anomalously dry seasons are selected. For dry years, the model is initiated in season 1 of 1984 and season 1 of 2008. For wet years, the model is initiated in season 1 of 1991 and season 1 of 1997. These simulations are run out for two years (six seasons total).

For the 1984 simulation, IWA is initially 11.4% lower for the first crop season with the forecast. The IWAs drop to zero for both of the second seasons due to the low storage, but the forecast simulation maintains a higher storage, which allowed for increased allocations for the following year, 1985. Total allocations over the two years are 383,050 acre-feet for the Forecast and 306,400 acre-feet for No-Forecast. A very similar pattern is visible in the simulation initiated in 2008 where once again total IWA is higher for the Forecast simulation (534,040 acre-

feet) when compared to No-Forecast (478,600 acre-feet) over short-term operations in response to low inflow years (Table 6).

For wet years, allocations are higher for three of the four crop seasons for the Forecast simulations. For 1997, total IWAs for the Forecast are 1,939,600 acre-feet and 1,522,500 acre-feet for No-Forecast. In response to the flooding in 1992, the Forecast simulation allocates 2,384,300 acre-feet to IWA while the No-Forecast simulation allocates 1,738,700 acre-feet (Table 6). This allows for more water to be used towards irrigation as opposed to being spilled.

Table 6: Extreme Year Simulation Results

	Year	IWA-Forecast (acre-feet)	IWA-No-Forecast (acre-feet)	Forecast Improvement
WET	1992	2,384,300	1,738,700	+37.1%
	1997	1,939,600	1,522,500	+27.4%
DRY	1984	383,050	306,400	+25.0%
	2008	534,040	478,600	+11.6%

When the simulations are initiated during seasons with anomalously low inflows, allocations for the forecast are initially lower. However by the second year, IWAs increase compared to No-Forecast and have larger total IWAs over the two year simulation due to higher storage. With simulations during flooding years, allocations are consistently higher. Thus in both cases of extreme events, allocations to irrigation are greater when the forecast is implemented over the course of short-term (two year) operation simulations.

3.3.4 Exceedance Probability Sensitivity Analysis

Failure probabilities of 5%, 25%, and 50% are analyzed within the objective function to assess impacts on interruptible water allocations. All of these

simulations are run as non-restricted and for the entire time duration. Generally, as the exceedance probability increases, the inflow volumes applied for Forecast and No-Forecast increases. With larger expected inflows, IWAs also increase (Table 7). With higher IWAs, the average combined storage decreases leading to lower reliabilities in meeting end of season target storage. Increasing the exceedance probability within the simulations increases IWAs, however the Forecast simulation consistently produces higher IWAs (10-12%) than the No-Forecast simulation. Therefore, a tradeoff exists when increasing the exceedance probability between increasing benefits (larger IWAs) and decreasing reliability.

Table 7: Failure Probability Sensitivity Analysis

Mean IWA (acre-feet)	$P_f = 5\%$	$P_f = 25\%$	$P_f = 50\%$
Forecast	225,310	252,980	289,460
No-Forecast	205,660	224,910	259,900

3.4 Discussion

Average values of evaporation rate were used within the iterative loop when calculating IWA. Average seasonal evaporation rates can vary by as much as 20%. Considering that average annual evaporation volume is 120,000 acre-feet, using accurate evaporation rate estimates is critical when optimizing IWA. By forecasting evaporation rates, through air temperature or wind data, it may be possible to improve upon estimating evaporation and allocate interruptible water supplies in a more optimal manner.

One issue with reliability-based allocations is that storage is attempting to reach the storage prescribed in the objective function. If storage is high in a given season, even if the forecast indicates much lower than average inflows, the model will still allocate a significant amount of water towards IWA as there is a fairly large margin between the preceding season storage and the end of season target storage. Numerous other optimization methods have been employed in water allocation optimization, such as stochastic dynamic programming or scenario tree based approaches (Watkins et. al., 2000, Stedinger et. al., 2013; Cote & Leconte, 2015) and warrant exploration. Another possible improvement to the study is to optimize over the entire time-series to determine the ideal or optimal IWA by season. This would assist in establishing new restrictions for maximum IWA.

The analysis for this study terminates in 2010, just prior to the historic Texas of 2011-2015. Further analysis is required to determine impact of a forecast during this unprecedented drought. It is possible that the forecast would have correctly predicted the below average inflows, leading to decreased IWAs initially with the Forecast approach. Once conditions become severe and reservoir levels drop below the target storage, the forecast has limited value. The utility of the drought may increase just prior to a return to normal conditions.

CHAPTER 4: Concluding Remarks

This thesis demonstrates a novel season-ahead hybrid autoregressive-principal component regression prediction model coupling both local and global predictor variables and its application to reservoir operations and water allocation within the LCRB in Texas. Predictors were initially identified based on findings of previous studies and correlation analysis. Multiple linear and logistic regression models are evaluated, with an application to the Highland Lakes reservoirs in central Texas. The superior predictor combination included ARMA model outputs, basin-wide soil moisture, CFSv2 precipitation predictions, and Equatorial Pacific SST information for the first crop season and ARMA, CFSv2, SLP and SST for the second crop season. The methodology developed here is transferable to other basins where large-scale climate teleconnections exist, and may help to skillfully inform water management and planning, fostering improved water allocation decision-making.

Despite the simplicity of using a reliability-based objective function to allocate interruptible water supplies, several benefits were identified based on simulation results. During wet seasons, Forecast simulations have higher water allocations than No-Forecast resulting in lower spill volume. During dry seasons, IWAs were larger for the No-Forecast simulation however analysis of short-term (two year) responses to extreme events reveals that Forecast simulations maintain a higher combined storage, which ultimately leads to larger total allocations in subsequent seasons. Over long-term operations, the forecast yielded reduced benefits when maximum IWA restrictions were imposed and also when combined storage was

low (< 1.3 million acre-feet) and both Forecast and No-Forecast simulations produced IWAs of zero acre-feet.

References

Akaike, Hirotogu. 1998. “Information Theory and an Extension of the Maximum Likelihood Principle.” In *Selected Papers of Hirotugu Akaike*, edited by Emanuel Parzen, Kunio Tanabe, and Genshiro Kitagawa, 199–213. Springer Series in Statistics. Springer New York. http://link.springer.com/chapter/10.1007/978-1-4612-1694-0_15.

Awadallah, A. G., and J Rousselle. 2000. “Improving Forecasts of Nile Flood Using SST Inputs in TFN Model.” *Journal of Hydrologic Engineering* 5 (4): 371–79. doi:10.1061/(ASCE)1084-0699(2000)5:4(371).

Block, Paul, and Balaji Rajagopalan. 2009. “Statistical–Dynamical Approach for Streamflow Modeling at Malakal, Sudan, on the White Nile River.” *Journal of Hydrologic Engineering* 14 (2): 185–96.

Box, George E. P., Gwilym M. Jenkins, and Gregory C. Reinsel. 2008. *Time Series Analysis: Forecasting and Control*. Wiley.

Can, İbrahim, Fatih Tosunoğlu, and Ercan Kahya. 2012. “Daily Streamflow Modelling Using Autoregressive Moving Average and Artificial Neural Networks Models: Case Study of Çoruh Basin, Turkey.” *Water and Environment Journal* 26 (4): 567–76. doi:10.1111/j.1747-6593.2012.00337.x.

Changnon, Stanley A., and Donald R. Vonnhame. 1986. “Use of Climate Predictions to Decide a Water Management Problem1.” *JAWRA Journal of the American Water Resources Association* 22 (4): 649–52. doi:10.1111/j.1752-1688.1986.tb01919.x.

Chiew, F. H. S., S. L. Zhou, and T. A. McMahon. 2003. “Use of Seasonal Streamflow Forecasts in Water Resources Management.” *Journal of Hydrology* 270 (1–2): 135–44. doi:10.1016/S0022-1694(02)00292-5.

Clifford, Michael J., Monique E. Rocca, Robert Delph, Paulette L. Ford, Neil S. Cobb, and others. 2008. “Drought Induced Tree Mortality and Ensuing Bark Beetle Outbreaks in Southwestern Pinyon-Juniper Woodlands.” In *Ecology, Management, and Restoration of Pinon-Juniper, and Ponderosa Pine Ecosystems: Combined Proc. of the 2005 St. George, Utah and 2006 Albuquerque, New Mexico Workshops*, 39–51. Citeseer. http://citeseerx.ist.psu.edu/viewdoc/download?doi=10.1.1.165.4291&rep=rep1&type=pdf#page=49.

Cook, Edward R., Richard Seager, Mark A. Cane, and David W. Stahle. 2007. “North American Drought: Reconstructions, Causes, and Consequences.” *Earth-Science Reviews* 81 (1–2): 93–134. doi:10.1016/j.earscirev.2006.12.002.

Côté, Pascal, and Robert Leconte. 2015. “Comparison of Stochastic Optimization Algorithms for Hydropower Reservoir Operation with Ensemble Streamflow Prediction.” *Journal of Water Resources Planning and Management*, 04015046.

Coulibaly, Paulin, François Anctil, Ramon Aravena, and Bernard Bobée. 2001. “Artificial Neural Network Modeling of Water Table Depth Fluctuations.” *Water Resources Research* 37 (4): 885–96. doi:10.1029/2000WR900368.

“ESRL : PSD : Climate Indices: Monthly Atmospheric and Ocean Time Series.” 2015. Accessed April 21. http://www.esrl.noaa.gov/psd/data/climateindices/list/.

Fernando, D. Nelun, Rong Fu, Ruben S. Solis, Robert E. Mace, Ying Sun, Binyan Yang, and Bing Pu. 2015. “Early Warning of Summer Drought over Texas and the South Central United States: Spring Conditions as a Harbinger of Summer Drought.” Technical Report 15-02. Ausin, TX: Texas Water Development Board. http://www.twdb.texas.gov/publications/reports/technical_notes/doc/TechnicalNote15-02.pdf.

Gámiz-Fortis, Sonia, David Pozo-Vázquez, Ricardo M. Trigo, and Yolanda Castro-Díez. 2008. “Quantifying the Predictability of Winter River Flow in Iberia. Part II: Seasonal Predictability.” *Journal of Climate* 21 (11): 2503–18. doi:10.1175/2007JCLI1775.1.

Gámiz-Fortis, S.R., J.M. Hidalgo-Muñoz, D. Argüeso, M.J. Esteban-Parra, and Y. Castro-Díez. 2011. “Spatio-Temporal Variability in Ebro River Basin (NE Spain): Global SST as Potential Source of Predictability on Decadal Time Scales.” *Journal of Hydrology* 409 (3-4): 759–75. doi:10.1016/j.jhydrol.2011.09.014.

Garen, David C. 1992. “Improved Techniques in Regression-Based Streamflow Volume Forecasting.” *Journal of Water Resources Planning and Management* 118 (6): 654–70. doi:10.1061/(ASCE)0733-9496(1992)118:6(654).

Golembesky, Kurt, A. Sankarasubramanian, and Naresh Devineni. 2009. “Improved Drought Management of Falls Lake Reservoir: Role of Multimodel Streamflow Forecasts in Setting up Restrictions.” *Journal of Water Resources Planning and Management* 135 (3): 188–97.

Hagedorn, Renate, Francisco J. Doblas-Reyes, and T. N. Palmer. 2005. “The Rationale behind the Success of Multi-Model Ensembles in Seasonal Forecasting – I. Basic Concept.” *Tellus A* 57 (3): 219–33. doi:10.1111/j.1600-0870.2005.00103.x.

Hamlet, A., D Huppert, and D. Lettenmaier, D. 2002. “Economic Value of Long-Lead Streamflow Forecasts for Columbia River Hydropower.” *Journal of Water Resources Planning and Management* 128 (2): 91–101. doi:10.1061/(ASCE)0733-9496(2002)128:2(91).

Hammer, Graeme L., Neville Nicholls, and Christopher Mitchell. 2000. *Applications of Seasonal Climate Forecasting in Agricultural and Natural Ecosystems: The Australian Experience*. Springer Science & Business Media.

Hoerling, Martin, Arun Kumar, Randall Dole, John W. Nielsen-Gammon, Jon Eischeid, Judith Perlwitz, Xiao-Wei Quan, Tao Zhang, Philip Pegion, and Mingyue Chen. 2012. “Anatomy of an Extreme Event.” *Journal of Climate* 26 (9): 2811–32. doi:10.1175/JCLI-D-12-00270.1.

IPCC. 2013. *Climate Change 2013: The Physical Science Basis. Contribution of Working Group I to the Fifth Assessment Report of the Intergovernmental Panel on Climate Change*. Cambridge, United Kingdom and New York, NY, USA: Cambridge University Press. www.climatechange2013.org.

Kalnay, E., M. Kanamitsu, R. Kistler, W. Collins, D. Deaven, L. Gandin, M. Iredell, et al. 1996. “The NCEP/NCAR 40-Year Reanalysis Project.” *Bulletin of the American Meteorological Society* 77 (3): 437–71. doi:10.1175/1520-0477(1996)077<0437:TNYRP>2.0.CO;2.

Karl, Thomas R., Jerry M. Melillo, Thomas C. Peterson, and U.S. Global Change Research Program. 2009. *Global Climate Change Impacts in the United States: A State of Knowledge Report*. Cambridge [England] ; New York: Cambridge University Press.

Koster, Randal D., Paul A. Dirmeyer, Zhichang Guo, Gordon Bonan, Edmond Chan, Peter Cox, C. T. Gordon, et al. 2004. “Regions of Strong Coupling Between Soil Moisture and Precipitation.” *Science* 305 (5687): 1138–40. doi:10.1126/science.1100217.

Krzysztofowicz, Roman. 2001. “The Case for Probabilistic Forecasting in Hydrology.” *Journal of Hydrology* 249 (1–4): 2–9. doi:10.1016/S0022-1694(01)00420-6.

Kwiatkowski, Denis, Peter C. B. Phillips, Peter Schmidt, and Yongcheol Shin. 1992. “Testing the Null Hypothesis of Stationarity against the Alternative of a Unit Root: How Sure Are We That Economic Time Series Have a Unit Root?” *Journal of Econometrics* 54 (1–3): 159–78. doi:10.1016/0304-4076(92)90104-Y.

LCRA. 2007. “Summer 2007 Flood Report.” Austin, TX: Lower Colorado River Authority. http://hydromet.lcra.org/riverreport/Documents/2007_Flood_Report.pdf.

Loucks, Daniel P., Jery R. Stedinger, and Douglas A. Haith. 1981. *Water Resource Systems Planning and Analysis*. Prentice-Hall.

McCabe, Gregory J., Michael A. Palecki, and Julio L. Betancourt. 2004. “Pacific and Atlantic Ocean Influences on Multidecadal Drought Frequency in the United States.” *Proceedings of the National Academy of Sciences* 101 (12): 4136–41. doi:10.1073/pnas.0306738101.

Mohan, S., and S. Vedula. 1995. “Multiplicative Seasonal Arima Model for Longterm Forecasting of Inflows.” *Water Resources Management* 9 (2): 115–26. doi:10.1007/BF00872463.

Morin, Jennifer, Paul Block, Balaji Rajagopalan, and Martyn Clark. 2008. “Identification of Large Scale Climate Patterns Affecting Snow Variability in the Eastern United States.” *International Journal of Climatology* 28 (3): 315–28. doi:10.1002/joc.1534.

North, Gerald R., Thomas L. Bell, Robert F. Cahalan, and Fanthune J. Moeng. 1982. “Sampling Errors in the Estimation of Empirical Orthogonal Functions.” *Monthly Weather Review* 110 (7): 699–706. doi:10.1175/1520-0493(1982)110<0699:SEITEO>2.0.CO;2.

Oglesby, Robert J., and David J. Erickson. 1989. “Soil Moisture and the Persistence of North American Drought.” *Journal of Climate* 2 (11): 1362–80. doi:10.1175/1520-0442(1989)002<1362:SMATPO>2.0.CO;2.

Piechota, Thomas C., and John A. Dracup. 1996. “Drought and Regional Hydrologic Variation in the United States: Associations with the El Niño-Southern Oscillation.” *Water Resources Research* 32 (5): 1359–73. doi:10.1029/96WR00353.

Quan, X., M. Hoerling, J. Whitaker, G. Bates, and T. Xu. 2006. “Diagnosing Sources of US Seasonal Forecast Skill.” *Journal of Climate* 19 (13): 3279–93.

Rajagopalan, Balaji, Edward Cook, Upmanu Lall, and Bonnie K. Ray. 2000. “Spatiotemporal Variability of ENSO and SST Teleconnections to Summer Drought over the United States during the Twentieth Century.” *Journal of Climate* 13 (24): 4244–55.

Ramos, M. H., S. J. van Andel, and F. Pappenberger. 2013. “Do Probabilistic Forecasts Lead to Better Decisions?” *Hydrology and Earth System Sciences* 17 (6): 2219–32. doi:10.5194/hess-17-2219-2013.

Rasmusson, Eugene M., Phillip A. Arkin, Wen-Yuan Chen, and John B. Jalickee. 1981. “Biennial Variations in Surface Temperature over the United States as Revealed by Singular Decomposition.” *Monthly Weather Review* 109 (3): 587–98. doi:10.1175/1520-0493(1981)109<0587:BVISTO>2.0.CO;2.

Regonda, Satish Kumar, Balaji Rajagopalan, Martyn Clark, and Edith Zagona. 2006. “A Multimodel Ensemble Forecast Framework: Application to Spring Seasonal Flows in the Gunnison River Basin.” *Water Resources Research* 42 (9): W09404. doi:10.1029/2005WR004653.

Saha, Suranjana, Shrinivas Moorthi, Xingren Wu, Jiande Wang, Sudhir Nadiga, Patrick Tripp, David Behringer, et al. 2013. “The NCEP Climate Forecast System Version 2.” *Journal of Climate* 27 (6): 2185–2208. doi:10.1175/JCLI-D-12-00823.1.

Salas, Jose D., and David R. Maidment. 1993. *Handbook of Hydrology*. McGraw-Hill.

Schepen, Andrew, Q. J. Wang, and David E. Robertson. 2012. “Combining the Strengths of Statistical and Dynamical Modeling Approaches for Forecasting Australian Seasonal Rainfall: STATISTICAL-DYNAMICAL RAINFALL FORECASTS.” *Journal of Geophysical Research: Atmospheres* 117 (D20): n/a – n/a. doi:10.1029/2012JD018011.

Seager, Richard, Yochanan Kushnir, Celine Herweijer, Naomi Naik, and Jennifer Velez. 2005. “Modeling of Tropical Forcing of Persistent Droughts and Pluvials over Western North America: 1856–2000*.” *Journal of Climate* 18 (19): 4065–88. doi:10.1175/JCLI3522.1.

Smith, Thomas M., Richard W. Reynolds, Thomas C. Peterson, and Jay Lawrimore. 2008. “Improvements to NOAA’s Historical Merged Land–Ocean Surface Temperature Analysis (1880–2006).” *Journal of Climate* 21 (10): 2283–96. doi:10.1175/2007JCLI2100.1.

Stedinger, Jery, Beth Faber, and Jonathan Lamontagne. 2015. “Developments in Stochastic Dynamic Programming for Reservoir Operation Optimization.” In *World Environmental and Water Resources Congress 2013*, 1266–78. American Society of Civil Engineers. Accessed July 30. http://ascelibrary.org/doi/abs/10.1061/9780784412947.125.

Stone, M. 1978. “Cross-Validation:a Review.” *Series Statistics* 9 (1): 127–39. doi:10.1080/02331887808801414.

Strzepek, Kenneth, Gary Yohe, James Neumann, and Brent Boehlert. 2010. “Characterizing Changes in Drought Risk for the United States from Climate Change.” *Environmental Research Letters* 5 (4): 044012. doi:10.1088/1748-9326/5/4/044012.

Sullivan, Johnny, and David R. Maidment. 2013. “Soil Moisture Mapping of Drought in Texas.” http://repositories.lib.utexas.edu/handle/2152/19752.

Thomas C. Pagano, Holly C. Hartmann. 2001. “Using Climate Forecasts for Water Management: Arizona and the 1997-1998 El Nino.” *JAWRA Journal of the American Water Resources Association* 37 (5): 1139–53. doi:10.1111/j.1752-1688.2001.tb03628.x.

Thomson, M. C., F. J. Doblas-Reyes, S. J. Mason, R. Hagedorn, S. J. Connor, T. Phindela, A. P. Morse, and T. N. Palmer. 2006. “Malaria Early Warnings Based on Seasonal Climate Forecasts from Multi-Model Ensembles.” *Nature* 439 (7076): 576–79. doi:10.1038/nature04503.

Ting, Mingfang, and Hui Wang. 1997. “Summertime U.S. Precipitation Variability and Its Relation toPacific Sea Surface Temperature.” *Journal of Climate* 10 (8): 1853–73. doi:10.1175/1520-0442(1997)010<1853:SUSPVA>2.0.CO;2.

Tootle, Glenn A., and Thomas C. Piechota. 2006. “Relationships between Pacific and Atlantic Ocean Sea Surface Temperatures and U.S. Streamflow Variability.” *Water Resources Research* 42 (7): W07411. doi:10.1029/2005WR004184.

Wang, D. C., and Jose D. Salas. 1991. *Forecasting Streamflow for Colorado River Systems*. Colorado Water Resources Research Institute, Colorado State University. http://www.cwi.colostate.edu/publications/cr/164.pdf.

Wang, W., J. K. Vrijling, TU Delft: Civil Engineering and Geosciences, and TU Delft, Delft University of Technology. 2006. “Stochasticity, Nonlinearity and Forecasting of Streamflow Processes.” IOS Press. http://resolver.tudelft.nl/uuid:d467b1a4-22ce-4009-b4cd-2c04dcd56d03.

Watkins, David W., Daene C. McKinney, Leon S. Lasdon, Soren S. Nielsen, and Quentin W. Martin. 2000. “A Scenario-Based Stochastic Programming Model for Water Supplies from the Highland Lakes.” *International Transactions in Operational Research* 7 (3): 211–30.

Wei, Wenge, and David W. Watkins. 2011. “Probabilistic Streamflow Forecasts Based on Hydrologic Persistence and Large-Scale Climate Signals in Central Texas.” *Journal of Hydroinformatics* 13 (4): 760. doi:10.2166/hydro.2010.133.

Wilks, Daniel S. 2011. *Statistical Methods in the Atmospheric Sciences, Volume 100, Third Edition*. 3 edition. Amsterdam ; Boston: Academic Press.

Yürekli, Kadri, Ahmet Kurunç, and Fazli Öztürk. 2005. “Testing the Residuals of an ARIMA Model on the Çekerek Stream Watershed in Turkey.” *Turkish Journal of Engineering and Environmental Sciences* 29 (2): 61–74.

Zhang, Zhihua, and Michael E. Mann. 2005. “Coupled Patterns of Spatiotemporal Variability in Northern Hemisphere Sea Level Pressure and Conterminous U.S. Drought.” *Journal of Geophysical Research: Atmospheres* 110 (D3): D03108. doi:10.1029/2004JD004896.